Development 140, 1594-1604 (2013) doi:10.1242/dev.090845

Floor plate-derived sonic hedgehog regulates glial and ependymal cell fates in the developing spinal cord

Kwanha Yu, Sean McGlynn and Michael P. Matise*

SUMMARY

Cell fate specification in the CNS is controlled by the secreted morphogen sonic hedgehog (Shh). At spinal cord levels, Shh produced by both the notochord and floor plate (FP) diffuses dorsally to organize patterned gene expression in dividing neural and glial progenitors. Despite the fact that two discrete sources of Shh are involved in this process, the individual contribution of the FP, the only intrinsic source of Shh throughout both neurogenesis and gliogenesis, has not been clearly defined. Here, we have used conditional mutagenesis approaches in mice to selectively inactivate Shh in the FP (Shh^{FP}) while allowing expression to persist in the notochord, which underlies the neural tube during neurogenesis but not gliogenesis. We also inactivated Smo, the common Hh receptor, in neural tube progenitors. Our findings confirm and extend prior studies suggesting an important requirement for Shh^{FP} in specifying oligodendrocyte cell fates via repression of Gli3 in progenitors. Our studies also uncover a connection between embryonic Shh signaling and astrocyte-mediated reactive gliosis in adults, raising the possibility that this pathway is involved in the development of the most common cell type in the CNS. Finally, we find that intrinsic spinal cord Shh signaling is required for the proper formation of the ependymal zone, the epithelial cell lining of the central canal that is also an adult stem cell niche. Together, our studies identify a crucial late embryonic role for Shh^{FP} in regulating the specification and differentiation of glial and epithelial cells in the mouse spinal cord.

KEY WORDS: Astrocytes, Ependymal zone, Hedgehog, Oligodendrocytes, Stem cells, Signaling center, Mouse

INTRODUCTION

During vertebrate embryogenesis, pattern formation and cell fate specification are directed by signaling centers that provide spatial information through the localized production and secretion of protein morphogens. In the developing central nervous system (CNS), regionalization begins at neural plate stages, when midline (future ventral) and lateral (future dorsal) signals initiate the organization of cell types along the transverse/dorsoventral (DV) axis. Ventral signals are provided by the secreted sonic hedgehog (Shh) protein, which is expressed sequentially in the embryonic node (or equivalent structure) during neurulation, then in its midline mesodermal derivative the notochord, and finally in the floor plate (FP), a group of non-neuronal ventral midline epithelial cells in the neural tube. Prior to and shortly after neural tube closure, the notochord is in direct contact with the ventral midline/FP region of the neural tube, but thereafter becomes displaced ventrally away from the spinal cord, thus leaving the FP as the only intrinsic source of Shh protein for the majority of neural and glial development. Despite this, very little is currently known about the unique and combined contributions of each tissue source of Shh to neural tube patterning and cell fate specification throughout embryogenesis.

Shh specifies ventral cell fates in the neural tube by controlling the expression of specific homeodomain (HD) or basic helix-loop-helix (bHLH) proteins in dividing progenitors (Dessaud et al., 2008; Jessell, 2000). Six ventral domains can be identified by gene expression patterns: the FP (Foxa2/Shh) (Dessaud et al., 2008), p3 (Nkx2.2), pMN (Olig2), p2 (Mash1, Foxn4), p1 (Dbx2), and p0 (Dbx1, Dbx2) domains, from ventral to dorsal. Shh regulates gene expression via the three Gli transcription factors (Jacob and Briscoe, 2003; Matise and Wang, 2011). Gli proteins have opposing effects on target genes: in the absence of Shh signaling, Gli3 is the primary transcriptional repressor produced by partial proteolysis, while Gli2 is largely degraded (Pan et al., 2006; Pan and Wang, 2007); whereas in cells exposed to Shh, Gli2/3 processing is blocked, and in their full-length form they function as transcriptional activators. The third Gli gene, *Gli1*, is a target of the pathway and is induced after signaling has commenced.

Shh regulates Gli processing via Ptch1 and Smo. In the absence of Shh, Ptch1 suppresses the pathway by inhibiting Smo, a seven-pass transmembrane protein that is absolutely required for all positive Hh signal transduction and which blocks the phosphorylation of Gli proteins that triggers their proteolytic processing (Dessaud et al., 2008). In *Shh* or *Smo* mutant cells, ventral progenitor markers and cell fates are not induced and dorsal genes become expressed ectopically (Chiang et al., 1996; Wijgerde et al., 2002). Notably, in both *Shh;Gli3* and *Smo;Gli3* double mutants in which no positive or negative Gli activity is present, most ventral cell fates are restored (except FP and p3 cells) (Litingtung and Chiang, 2000; Wijgerde et al., 2002). Together, these data show that a key role for Shh signaling is to block the formation of Gli3 repressors (Gli-R) in ventral cells in addition to inducing Gli activators (Gli-A) for target gene induction.

Prior studies have addressed the timing of Shh signaling during early neural development. In one elegant experiment, a mouse line expressing a GFP-tagged Shh fusion protein was created using gene targeting to allow direct visualization of the secreted protein in target tissues during embryogenesis (Chamberlain et al., 2008). It was shown that Shh-GFP protein can be detected at the lumenal surface of cells lining the ventral ventricular zone (VZ) even before Shh expression becomes induced in FP cells. These data, together with earlier analyses of patterning and cell fate specification defects

Department of Neuroscience and Cell Biology, UMDNJ/Robert Wood Johnson Medical School, 675 Hoes Lane, Piscataway, NJ 08840, USA.

*Author for correspondence (matisemp@umdnj.edu)

Accepted 21 January 2013

in mouse *Gli2* mutants that lack both FP and p3 cells (Ding et al., 1998; Lei et al., 2004; Matise et al., 1998), suggest that the earlier notochord-derived (Shh^{NOTO}) or node-derived Shh signals are sufficient to set up the initial pattern of progenitor gene expression in mice. These and other (Dessaud et al., 2010) results also suggest that Shh derived from the FP (Shh^{FP}) might play a more limited role in maintaining gene expression patterning set up by earlier sources. However, whether Shh^{FP} has a more specific or significant role during later stages of neural tube development, while gliogenesis and the terminal differentiation of multiple cell types are occurring, has not yet been determined.

The current study addresses this question using a conditional mutagenesis strategy to specifically block the ability of spinal cord cells to produce Shh or respond to Hh signaling during the period of development when the FP is the only intrinsic, local source of ligand. To do this we made use of conditional loxP-targeted ('floxed') *Shh* and *Smo* alleles and three different transgenic *Cre* recombinase-expressing lines that induce genetic deletions specifically in FP or spinal cord VZ progenitor cells at a time shortly after neural tube closure. Our analysis of mutant embryos at early stages confirms prior studies showing that Shh^{FP} is required to maintain progenitor gene expression in distinct VZ domains during neurogenesis. By contrast, at later stages during gliogenesis we find that Shh^{FP} is required for normal oligodendrocyte (OL) specification and does so by continually repressing the formation of Gli3-R in OL progenitor cells (OPCs), which inhibits Olig2 expression and OL specification. In addition, we provide evidence for active Shh-Gli signaling in embryonic ventral astrocyte progenitors in the mouse spinal cord and show that, in the absence of Shh^{FP} or signal transduction in progenitors, S100 expression is lost during embryogenesis and Gfap expression is upregulated abnormally in postnatal gray matter (protoplasmic) astrocytes, suggesting a possible role for Hh signaling in normal astrocyte maturation or function. Finally, we show that the ependymal zone surrounding the central canal, which has been shown to be an adult stem cell niche in rodents (Johansson et al., 1999), does not form properly in the absence of Shh signaling. Together, our findings reveal the cell type-specific requirements for intrinsic Shh signaling during spinal cord development in mice.

MATERIALS AND METHODS

Animals

To generate a FP-specific deletion of *Shh* ($Shh^{\Delta FP/\Delta FP}$), we crossed floxed *Shh* mice ($Shh^{flox/+}$) [Jackson Laboratory (Dassule et al., 2000)] with two different transgenic *Cre* lines: $Foxa2^{FP\text{-}CRM}::Cre$ and $Nkx2.2^{p3\text{-}CRM}::Cre$ (Wang et al., 2011). To generate $Smo^{\Delta NT/\Delta NT}$ mice lacking Smo in VZ cells, we crossed floxed *Smo* mice ($Smo^{flox/+}$) [Jackson Laboratory) (Long et al., 2001)] with *Nestin::Cre* mice [Jackson Laboratory (Tronche et al., 1999)]. To generate $Smo^{\Delta NT\text{-}V/\Delta NT\text{-}V}$ mice lacking *Smo* in the FP/p3/pMN domains, we crossed $Smo^{flox/+}$ mice with $Nkx2.2^{p3\text{-}CRM}::Cre$ mice. $Shh^{\Delta FP/\Delta FP};Gli3$ double mutants were generated using the *extra toes* allele ($Gli3^{xt}$) (Hui and Joyner, 1993). The following reporter lines were also used: *ROSA26-floxed-stop-lacZ* ($Rosa^{lz}$) (Soriano, 1999), *ROSA26-floxed-stop-EFYP* ($Rosa^{EYFP}$) (Srinivas et al., 2001) and $Gli1^{lacZ}$ (Bai et al., 2002).

Immunohistochemistry (IHC) and RNA *in situ* hybridization (ISH)

Staining of 14-16 μm cryostat sections using fluorochrome-conjugated secondary antibodies was performed as described (Lei et al., 2004). Primary antibodies were: mouse anti-Foxa2 (clone 4C7, DSHB, 1:100), anti-Nkx2.2 (clone 74.5A5, DSHB, 1:100), anti-Pax6 (DSHB, 1:100), anti-HB9 (clone 18.5C10, DSHB, 1:500) and anti-Shh (DSHB, Iowa City, IA, USA); rabbit anti-activated caspase 3 (BD Pharmigen, 1:500), mouse anti-Mash1/2 (BD Pharmingen, 1:100) and rat anti-Pdgfrα (BD Pharmigen, 1:1000); mouse anti-Apc (clone CC1, Millipore, 1:100); chicken anti-β-gal (abcam, 1:1000), anti-GFP, rat anti-BrdU (Abcam, 1:250); rabbit anti-Chx10 (a gift from R. McInnes, University of Toronto, Ontario, Canada); mouse anti-Gfap (Cell Signaling Technology, 1:1000); guinea pig anti-Gli2 [1:1000, a gift from J. Eggenschwiler, Princeton University, Princeton, NJ, USA (Cho et al., 2008)]; rabbit anti-Gli3 [1:100, clone 2676; a gift from S. Scales, Genentech, San Francisco, CA, USA (Wen et al., 2010)]; rabbit anti-Isl1/2 (clone K5, 1:5000; a gift from Tom Jessell, Columbia University, New York, NY, USA), rabbit anti-Nkx2.2 (a gift from Tom Jessell, 1:4000) and rabbit anti-Nkx6.1 (a gift from Tom Jessell, 1:8000); rabbit anti-Lmx1a (1:1000, a gift from M. German, UCSF, San Francisco, CA, USA); chicken anti-Mbp (Aves Labs, Tigard, OR, USA; 1:250); rabbit anti-Nfia (1:1000; a gift from B. Deneen, Baylor College of Medicine, Houston, TX, USA); rabbit anti-Olig2 (1:6000; a gift from H. Takebayashi, Kyoto University, Kyoto, Japan); rabbit anti-Pax6 (1:1000; Chemicon, Billerica, MA, USA); rabbit anti-phospho-histone H3 (1:5000; PHH3; Upstate Biotechnology, Lake Placid, NY, USA); rabbit anti-S100 (Dako, 1:400); rabbit anti-Sox2 and chicken anti-vimentin (Millipore; 1:1000); rabbit anti-Sox9 (1:2000; a gift from M. Wegner, University of Erlangen–Nürnberg, Bavaria, Germany) (Stolt, et al., 2003) and guinea pig anti-Sox10 (1:1000; a gift from M. Wegner) (Maka, et al., 2005); and anti-fluoromyelin (1:300, Invitrogen).

X-gal staining and RNA ISH were performed as previously described (Lei et al., 2004). RNA *in situ* probes were *Ptch1* (M. Scott, Stanford University, CA, USA), *Shh* exon 2 (D. Epstein, University of Pennsylvania, Philadelphia, PA, USA), *Mmd2* and *Fgfbp3* (B. Deneen).

RESULTS

Notochord regression is complete prior to gliogenesis in the spinal cord

To address the unique role of floor plate-derived Shh (Shh^{FP}) in the mouse spinal cord, we mapped the separation of the notochord (regression) from direct contact with the neural tube in wild-type (WT) embryos (Fig. 1A). At embryonic day (E) 9.5 (24-25 somites) (n=6), the notochord is still in contact with ventral midline cells at all spinal cord levels. In 26- to 28-somite embryos (n=5), the notochord was not in contact with the neural tube at the level of somites 1-2. In 30-somite embryos (n=4), regression has progressed caudally beyond the forelimb buds located adjacent to somites 6-11. In 38-somite (~E10.5) embryos (n=4), regression reached the hindlimb buds (at somite levels 23-28). At the 42-somite stage (~E11), notochord regression has progressed beyond the hindlimb buds into sacral levels (n=4 embryos). Thus, the notochord is no longer in contact with the overlying neural tube at forelimb levels in E10.5 embryos and at neither the forelimb nor hindlimb level at E11.5, and it takes ~48 hours for regression to occur along the length of the spinal cord once it begins at cervical levels at ~E9.5 (Fig. 1B).

Conditional deletion of *Shh* in floor plate cells

Our results indicate that notochord regression takes place during neurogenesis and is complete prior to the onset of gliogenesis at spinal cord levels (Fig. 1B). To determine the requirement of Shh^{FP} for neurogenesis and gliogenesis, we generated embryos with conditional inactivation of Shh specifically in FP ($Shh^{\Delta FP}$) but not notochord (Shh^{NOTO}) cells using a conditional floxed *Shh* mouse line ($Shh^{flox/flox}$) (Dassule et al., 2000). To control for potential differences between the timing, levels and extent of expression of gene regulatory elements, we used two distinct transgenic lines to drive Cre expression specifically in ventral midline precursors, including FP progenitors, shortly after neural tube closure but prior to the induction of Shh expression. The first employed the FP cis-regulatory module (CRM) from the *Foxa2* gene to drive *Cre* in a transgenic line (designated $Foxa2^{FP\text{-}CRM}::Cre$), whereas the second line used the CRM from the p3 progenitor marker *Nkx2.2* (designated $Nkx2.2^{p3\text{-}CRM}::Cre$) (Sasaki and Hogan, 1996; Wang et al., 2011; Lei et al., 2006). Published work mapping the expression of Cre from these two CRMs using the *ROSA26-floxed-stop-lacZ* ($Rosa^{lz}$) reporter

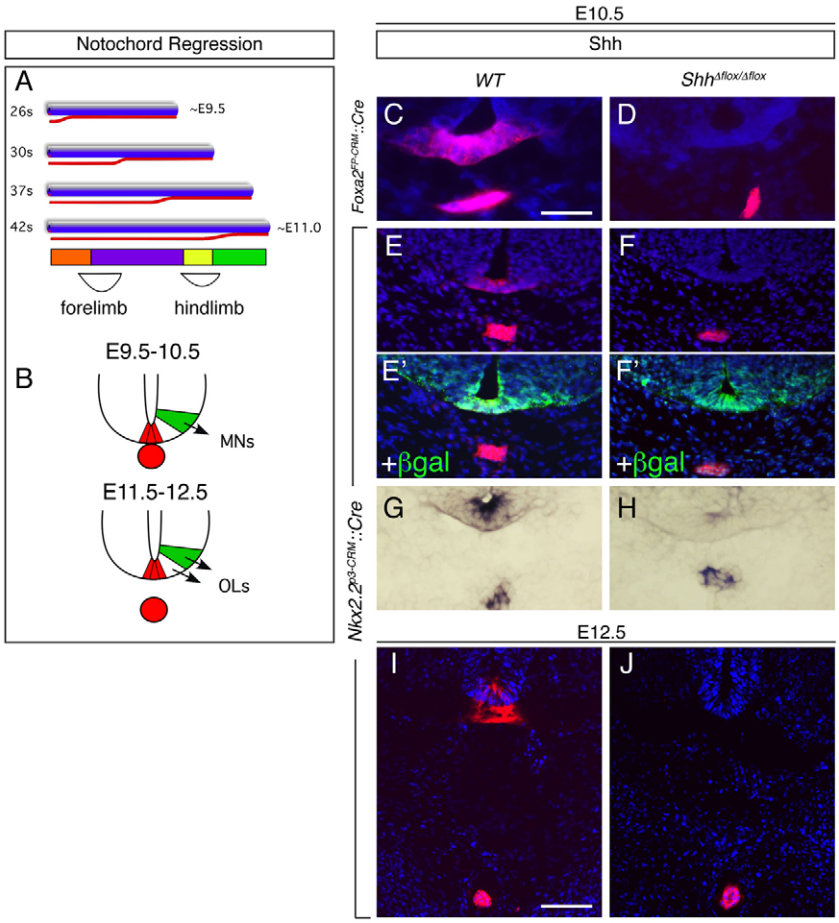

Fig. 1. Notochord regression in mice and conditional deletion of floor plate Shh (Shh^{FP}) prior to gliogenesis. (**A**) Schematic showing the movement of the notochord (red bar) away from direct contact with the ventral neural tube (blue rod) between the 26- and 42-somite stages (corresponding to ~E9.5 to E11.5) in the mouse embryo. Bars at the bottom indicate the relative position of the cervical (red), thoracic (purple), lumbar (yellow) and sacral (green) spinal cord regions in relation to the developing forelimb and hindlimb buds. (**B**) Schematics depicting a transverse view of the ventral spinal cord at neurogenic (top) and gliogenic (bottom) embryonic stages, showing the position of the notochord (red circle) relative to the ventral midline floor plate (red wedge). Motoneurons (MNs) (green wedge) are generated during neurogenesis, whereas later during gliogenesis these same regions generate oligodendrocytes (OLs) and astrocytes. (**C-J**) Selective conditional deletion of Shh^{FP}. Shh protein and *Shh* gene expression are not detected in the ventral neural tube of E10.5 (C-H) or E12.5 (I,J) embryos with conditional inactivation in FP cells (*Shh*$^{\Delta FP/\Delta FP}$) using the *Foxa2*$^{FP\text{-}CRM}$*::Cre* or *Nkx2.2*$^{p3\text{-}CRM}$*::Cre* transgenic lines. Note normal notochord regression in *Shh*$^{\Delta FP/\Delta FP}$ embryos. (C-F′) Expression of Shh protein at E10.5 in WT (C,E,E′) and *Shh*$^{\Delta FP/\Delta FP}$ mutants (D,F,F′). Embryos in E′ and F′ express β-gal from the *Rosa*^{lz} conditional reporter line and show that *Nkx2.2*$^{p3\text{-}CRM}$-driven Cre expression does not depend on Shh^{FP}. (G,H) Localization of *Shh* mRNA in WT and *Nkx2.2*$^{p3\text{-}CRM}$*::Cre;Shh*$^{\Delta FP/\Delta FP}$ embryos. (I,J) Shh protein expression at E12.5. Scale bars: 50 μm.

line (Soriano, 1999) showed that the expression of *Foxa2*$^{FP\text{-}CRM}$*::Cre* is restricted to FP cells, whereas *Nkx2.2*$^{p3\text{-}CRM}$*::Cre* labels all cells in the FP and p3 lineages and ~90% of pMN cells (Wang et al., 2011). Furthermore, neither enhancer requires Shh^{FP} for expression (Fig. 1E′,F′; data not shown).

To confirm the specificity of the deletion, we examined Shh protein and *Shh* mRNA expression in *Shh*$^{\Delta FP/\Delta FP}$ embryos generated with both Cre driver lines at E10.5 (Fig. 1C-H) and E12.5 (Fig. 1I,J). *Shh* expression was detected in the notochord but never in the ventral midline FP region of the ventral neural tube in either line. Importantly, notochord regression was not affected by the absence of Shh^{FP} (Fig. 1D,F,J), unlike other mouse mutants lacking Shh^{FP} (Matise et al., 1998). We then determined whether the absence of Shh^{FP} alters the expression of Shh target genes in the ventral neural tube by examining *Ptch1* and *Gli1* (Jeong and McMahon, 2005; Bai et al., 2002). *Ptch1* expression was reduced in the spinal cord at both E10.5 and E12.5 in *Nkx2.2*$^{p3\text{-}CRM}$*::Cre;Shh*$^{\Delta flox/\Delta flox}$ embryos (supplementary material Fig. S1A-D), but was not affected in the gut, which does not express Cre from *Nkx2.2*$^{p3\text{-}CRM}$ (data not shown). *Gli1* expression was determined by examining β-gal reporter expression from a *lacZ* knock-in to the *Gli1* locus (*Gli1*^{lacZ}) (Bai et al., 2002). *Gli1* expression was also reduced in the spinal cord, but not in migrating sclerotomal cells that do not express Cre (supplementary material Fig. S1E,F). By contrast, the expression of a Shh pathway-independent FP marker, Lmx1a, was unaffected (supplementary material Fig. S1G,H). These data show that loss of Shh^{FP} in the neural tube is required to maintain Shh-Gli target gene expression and that the levels of signaling are reduced in the ventral neural tube in the absence of this source.

It has been reported that *Shh*$^{-/-}$ mutants exhibit a severe reduction in the overall size of the neural tube and a widespread increase in cell death in dorsal and ventral cells (Borycki et al., 1999; Litingtung and Chiang, 2000). Although we did not detect changes in cell cycle or cell death markers in either line at E10.5 or E12.5 (supplementary material Fig. S2; data not shown), the gray matter area of the spinal cord in *Shh*$^{\Delta FP/\Delta FP}$ embryos was reduced compared with WT at E15.5 and E18.5 by 16% and 22%, respectively (data not shown). In addition, *Shh*$^{\Delta FP/\Delta FP}$ embryos did not display the characteristic CNS phenotypes, such as holoprosencephaly or cyclopia, that typify mouse mutants with reduced Shh signaling (Chiang et al., 1996) (data not shown). Thus, even though earlier (node or notochord) sources appear to be largely sufficient to prevent early apoptosis and maintain cell cycle dynamics, our data indicate that there is an ongoing requirement for Shh^{FP} to support spinal cord growth during development.

Shh^{FP} is required to maintain specific neural progenitor domain cell numbers

To investigate the effect of the loss of Shh^{FP} on the patterning and specification of progenitor cell fates in the ventral neural tube, we analyzed the expression of specific HD and bHLH transcription factors in *Shh*$^{\Delta FP/\Delta FP}$ mutants at E10.5. We restricted our analysis to thoracic/forelimb bud levels in staged E10.5 embryos (with 32-35 somites) in which notochord regression had recently occurred (see Fig. 1). Quantitatively similar data were obtained in *Foxa2*$^{FP\text{-}CRM}$ and *Nkx2.2*$^{p3\text{-}CRM}$ transgenic Cre lines, indicating that any minor differences in their spatiotemporal expression profiles are

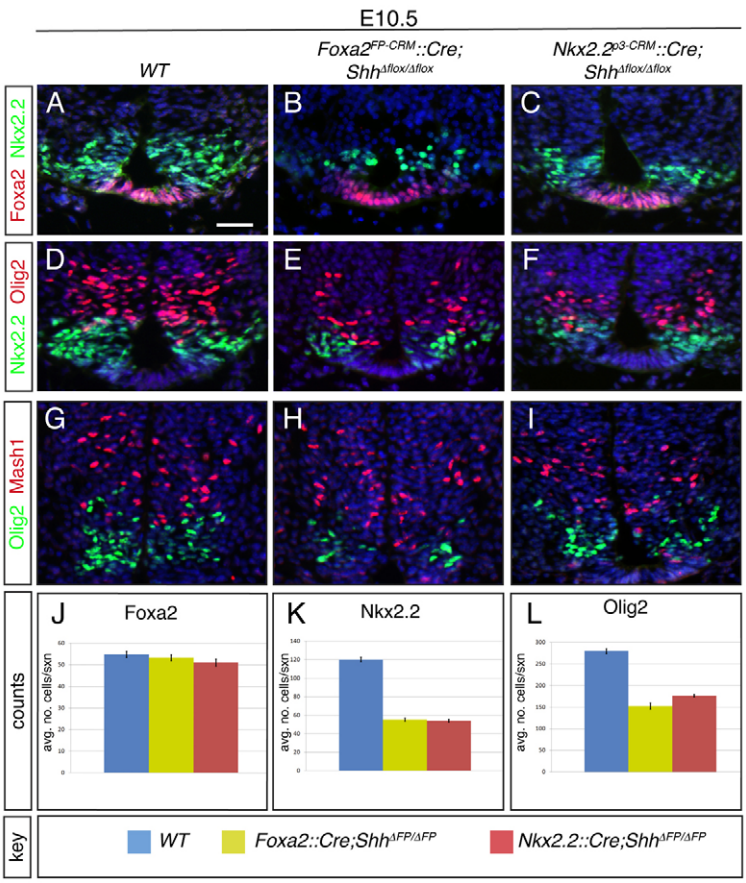

Fig. 2. Altered progenitor domain marker protein expression in $Shh^{\Delta FP/\Delta FP}$ embryos at E10.5. (**A-C**) Foxa2 (FP) and Nkx2.2 (p3) expression in WT, $Foxa2^{FP\text{-}CRM}::Cre;Shh^{\Delta flox/\Delta flox}$ and $Nkx2.2^{p3\text{-}CRM}::Cre;Shh^{\Delta flox/\Delta flox}$ transgenic lines. (**D-F**) Olig2 (pMN) and Nkx2.2 (p3) expression. (**G-I**) Olig2 (pMN) and Mash1 (p2) expression. (**J-L**) Cell counts for Foxa2, Nkx2.2 and Olig2. Error bars indicate s.e.m. Scale bar: 50 μm.

irrelevant for deleting Shh^{FP}, and that they can be used interchangeably for this purpose (Fig. 2J-L). Analysis of Foxa2 (FP), Nkx2.2 (p3), Olig2 (pMN) and Mash1 (Ascl1 – Mouse Genome Informatics) (p2) expression revealed a specific pattern of changes. Whereas the number of $Foxa2^+$ cells was not altered compared with WT (Fig. 2A-C,J), there was a significant reduction in $Nkx2.2^+$ and $Olig2^+$ cells at this stage (55% and 34%, respectively; Fig. 2A-F,K,L). Also, the number of $Mash1^+$ p2 progenitors was reduced in $Shh^{\Delta FP/\Delta FP}$ mutants (by ~27%) (Fig. 3G-I). Taken together, these results are consistent with previous data suggesting that the Shh signaling that occurs prior to FP induction is sufficient to generate the proper pattern of ventral progenitor gene expression (Matise et al., 1998; Jeong and McMahon, 2005), whereas ongoing Shh signaling from the FP is necessary to maintain progenitor domain formation during neurogenesis (Dessaud et al., 2010). Furthermore, since the phenotypes were very similar in both $Foxa2^{FP\text{-}CRM}::Cre;Shh^{\Delta flox/\Delta flox}$ and $Nkx2.2^{p3\text{-}CRM}::Cre;Shh^{\Delta flox/\Delta flox}$ mutants, all subsequent $Shh^{\Delta FP/\Delta FP}$ data was generated using the latter line.

To determine the impact of the changes seen during neurogenesis on later stages, we examined progenitor protein expression at E11.5 in embryos with more than 42 somites (supplementary material Fig. S3). At this stage, notochord regression has occurred at the forelimb bud level ~48 hours earlier and at the hindlimb bud levels ~12-24 hours earlier (Fig. 1A). Consistent with the E10.5 data, we saw no change in Foxa2 expression at either axial level. By contrast, there was a ~50% reduction in $Nkx2.2^+$ cells as compared with WT tissue in thoracic regions, and at lumbar levels it was slightly attenuated (37% reduction) (supplementary material Fig. S3A,C,D,F,G,I-K). Interestingly, the number of $Olig2^+$ cells was dramatically different in the two regions, with thoracic regions more severely affected than lumbar: 92% versus 56% reductions, respectively, compared with WT embryos (supplementary material Fig. S3D-I,L). Since the notochord regresses ~24 hours earlier in thoracic than lumbar regions (Fig. 1), these observations suggest a crucial role for Shh^{FP} in maintaining *Olig2* expression in thoracic pMN cells between E10.5 and E11.5.

We next examined $Shh^{\Delta FP/\Delta FP}$ mutants at E12.5. Similar to results from E10.5 and E11.5, no significant changes were seen in $Foxa2^+$ cells in $Shh^{\Delta FP/\Delta FP}$ embryos (Fig. 3A,B,M). For Nkx2.2, we found a similar decrease in the number of $Nkx2.2^+$ cells (~25%) to that seen at E11.5 (Fig. 3A,B,D,E,N). By contrast, in $Shh^{\Delta FP/\Delta FP}$ mutants, few if any $Olig2^+$ cells were detected in either thoracic or lumbar levels at this stage (Fig. 3D,E,O; data not shown). This loss was accompanied by a ventral shift in the position of postmitotic $Chx10^+$ (Vsx2 – Mouse Genome Informatics) V2 interneurons, which normally derive from the p2 domain immediately dorsal to motoneurons (MNs) (Fig. 3G,H). Lineage-tracing experiments using the $Rosa^{lz}$ conditional *lacZ* reporter revealed that many $Chx10^+$ cells were $\beta\text{-gal}^+$ in $Nkx2.2^{p3\text{-}CRM}::Cre;Shh^{\Delta FP/\Delta FP};Rosa^{lz}$ mutants (Fig. 3J,K), suggesting that some pMN cells transfate into p2 cells in the absence of Olig2 expression in $Shh^{\Delta FP/\Delta FP}$ mutant embryos. Thus, Shh^{FP} is required to maintain *Olig2* expression in lumbar pMN cells between E11.5 and E12.5.

It has been shown that MN specification requires Olig2 (Lu et al., 2002). Thus, to determine whether the progressive loss of Olig2 between E10.5 and E11.5 in $Shh^{\Delta FP/\Delta FP}$ mutants compromised MN differentiation, we examined expression of HB9 (Mnx1 – Mouse Genome Informatics), islet 1/2 (Isl1/2) and Lim1 (Lhx1 – Mouse Genome Informatics) at E12.5 and E13.5 (supplementary material Fig. S4; data not shown). The number of $HB9^+$ and $Isl1/2^+$ cells was

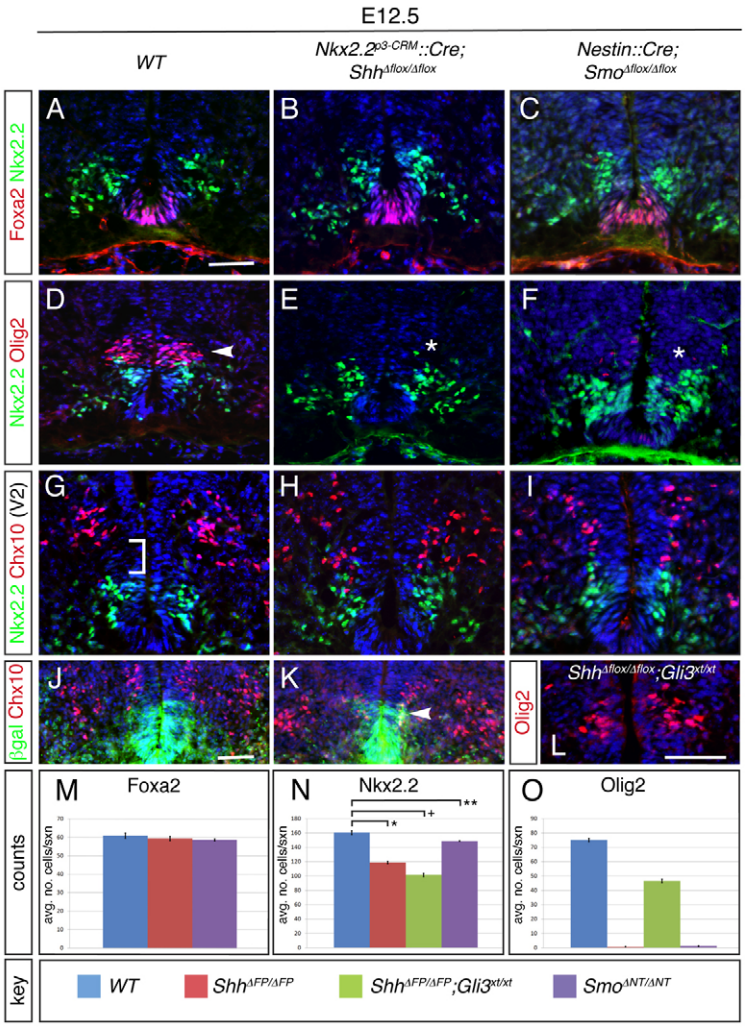

Fig. 3. Altered progenitor domain marker protein expression in $Shh^{\Delta FP/\Delta FP}$ embryos at E12.5. (**A-C**) Foxa2 (FP) and Nkx2.2 (p3) expression in WT, $Nkx2.2^{p3\text{-}CRM}$*::Cre;*$Shh^{\Delta flox/\Delta flox}$ and *Nestin::Cre;*$Smo^{\Delta flox/\Delta flox}$ transgenic lines. (**D-F**) Olig2 (pMN) and Nkx2.2 (p3) expression at lumbar levels. Note the absence of Olig2 expression (arrowhead in D indicates expression in WT) in $Shh^{\Delta FP/\Delta FP}$ and $Smo^{\Delta NT/\Delta NT}$ embryos (asterisks). (**G-I**) Chx10 (V2a interneurons) and Nkx2.2 expression. Bracket in G indicates the pMN domain (located between the p3 and p2 domains) in WT embryos that is absent in $Shh^{\Delta FP/\Delta FP}$ or $Smo^{\Delta NT/\Delta NT}$ embryos. (**J**,**K**) Expression of Chx10 and β-gal in $Nkx2.2^{p3\text{-}CRM}$*::Cre* mice. In WT embryos, $Chx10^+$ cells are generated from the p2 lineage that does not activate expression of $Nkx2.2^{p3\text{-}CRM}$ (as indicated by β-gal expression) (Wang et al., 2011), whereas in $Shh^{\Delta FP/\Delta FP}$ embryos lacking Olig2 expression some $Chx10^+$ cells co-express β-gal (K, yellow cells, arrowhead). (**L**) Expression of Olig2 is substantially rescued in $Nkx2.2^{p3\text{-}CRM}$*::Cre;*$Shh^{\Delta flox/\Delta flox}$*;*$Gli3^{xt/xt}$ mice that also lack *Gli3*. Thoracic level is shown. (**M-O**) Cell counts for each marker for the indicated genotypes. $^{**}P$=0.07; $^{*}P$<0.001; ^{+}P<0.0001. Student's two-tailed *t*-test. Error bars indicate s.e.m. Scale bars: 50 μm.

reduced in $Shh^{\Delta FP/+}$ and $Shh^{\Delta FP/\Delta FP}$ embryos compared with WT littermates (supplementary material Fig. S4). This finding is consistent with an ongoing requirement for Shh^{FP} for the generation of normal numbers of MNs in the spinal cord.

Shh^{NOTO} does not influence spinal cord cell fates after E12.5

Our results suggest that Shh^{FP} is required to maintain Olig2 expression between E10.5 and E12.5 when the notochord is no longer in contact with the spinal cord. To determine whether Shh from the regressing notochord (or other sources) could still influence cell fate, we compared the phenotypes of $Shh^{\Delta FP/\Delta FP}$ mutants with those of embryos with conditional inactivation of *Smo* in the neural tube ($Smo^{\Delta NT}$) that were generated using the nestin CRM to drive Cre (*Nestin::Cre*) (Tronche et al., 1999) and a conditional floxed *Smo* allele (Smo^{flox}) (Long et al., 2001). We reasoned that if Shh^{NOTO} or other Hh ligands were able to partially compensate for the loss of Shh^{FP}, we would see a more severe phenotype in conditional $Smo^{\Delta NT/\Delta NT}$ than in $Shh^{\Delta FP/\Delta FP}$ mutants.

Analysis of progenitor gene expression in E12.5 *Nestin::Cre;*$Smo^{\Delta flox/\Delta flox}$ ($Smo^{\Delta NT/\Delta NT}$) embryos revealed an overall pattern similar to that of $Shh^{\Delta FP/\Delta FP}$ mutants: the number of $Foxa2^+$ cells was similar to WT in $Smo^{\Delta NT/\Delta NT}$ mutants, whereas $Olig2^+$ cells were almost entirely absent (Fig. 3C,F; data not shown). Loss of Olig2 was accompanied by a ventral shift in the position of $Chx10^+$ V2 interneurons in $Smo^{\Delta NT/\Delta NT}$ embryos (Fig. 3I). Interestingly, the number of $Nkx2.2^+$ cells in $Smo^{\Delta NT/\Delta NT}$ embryos was more similar to that of the WT, with only 7% fewer cells than WT (Fig. 3C,F,I,N). These subtle differences might be attributable to the slightly later timing of Cre expression from the nestin promoter compared with the $Nkx2.2^{p3CRM}$ used to remove *Shh* from the FP (data not shown). Despite this, these data provide evidence that additional sources of Hh ligands do not influence spinal cord ventral progenitor gene expression between E10.5 and E12.5 and that Shh^{FP} is the sole source required during this period.

Shh^{FP} maintains Olig2 in part by inhibiting Gli3 repressor activity

It has been shown previously that many of the phenotypes of *Shh* mutants can be rescued by genetically removing *Gli3* (Litingtung and Chiang, 2000; Rallu et al., 2002), indicating that derepression of Gli3-mediated target gene expression is a key element of Shh signaling. To test whether the loss of *Gli3* could rescue $Olig2^+$ cells in $Shh^{\Delta FP/\Delta FP}$ mutants, we generated $Shh^{\Delta FP/\Delta FP}$*;*$Gli3^{xt/xt}$ double mutants. $Shh^{\Delta FP/\Delta FP}$*;*$Gli3^{xt/xt}$ embryos (n=3) showed a partial rescue in *Olig2* expression at E12.5 (Fig. 3L,O). In contrast to $Shh^{\Delta FP/\Delta FP}$ mutants, which exhibited a 99% reduction in $Olig2^+$ cells, double mutants had only a 38% decrease (Fig. 3O). Furthermore, staining for Gli3 protein demonstrated a notable upregulation of expression in the Olig2-generating pMN domain in both $Shh^{\Delta FP/\Delta FP}$ and

Smo$^{\Delta NT/\Delta NT}$ tissue sections (supplementary material Fig. S5). Thus, Shh^{FP} maintains *Olig2* expression in part by blocking Gli3-R activity. By contrast, Nkx2.2 expression was not rescued in *Shh*$^{\Delta FP/\Delta FP}$;*Gli3*$^{xt/xt}$ double mutants at E12.5; in fact, 15% fewer cells were detected compared with *Shh*$^{\Delta FP/\Delta FP}$ mutants alone (Fig. 3N). Since Nkx2.2 expression requires Gli-A proteins (Bai et al., 2004; Lei et al., 2004), this finding supports the idea that Shh^{FP} is required to maintain Gli3-A to partially support the induction of Nkx2.2 in *Shh*$^{\Delta FP/\Delta FP}$;*Gli3*$^{xt/xt}$ double-mutant embryos.

Shh^{FP} is required for oligodendrocyte specification during gliogenesis

To further investigate the genetic pathway involved in maintaining Olig2 expression in glial progenitors, we examined the expression of several genes that have been linked to gliogenesis (Kang et al., 2012). Among those examined, expression of fibroblast growth factor binding protein 3 (*Fgfbp3*) and monocyte to macrophage differentiation-associated 2 (*Mmd2*) was reduced in E12.5 *Shh*$^{\Delta FP/\Delta FP}$ and *Smo*$^{\Delta NT/\Delta NT}$ mutants and restored in *Shh*$^{\Delta FP/\Delta FP}$;*Gli3*$^{xt/xt}$ double-mutant embryos (supplementary material Fig. S6), an expression profile similar to that of other Shh-Gli pathway-regulated genes, such as *Olig2* (Matise and Wang, 2011). Notably, expression of the Sox9 and nuclear factor 1A (Nfia) transcription factors, which have been shown to be required for the expression of *Mmd2* in chick embryos (Kang et al., 2012), was not affected in any mutant line (supplementary material Fig. S6), further supporting the possibility that *Mmd2* might be a direct target of Gli3-R in developing glial progenitors in the spinal cord.

The changes in glial progenitor markers at E11.5-12.5 indicate that OL specification might be perturbed in mutant embryos. To study this, we examined OPC marker expression in white matter (WM) tracts in E15.5 and E18.5 *Shh*$^{\Delta FP/\Delta FP}$ mutants stained with antibodies against Nkx2.2, Olig2, Sox10 and platelet-derived growth factor receptor alpha (Pdgfrα). We focused our attention on two WM regions: the dorsal funiculus (DF) and ventral funiculus (VF). As expected by the loss of Olig2 expression at E12.5, the number of Olig2^{+} OPCs in E15.5 *Shh*$^{\Delta FP/\Delta FP}$ mutants was decreased in the DF and VF by 70% and 90%, respectively (Fig. 4A,B,E,F,Q,R). Similarly, the number of cells expressing Nkx2.2, Sox10 and Pdgfrα was also severely reduced in both WM regions (Fig. 4A,B,E,F,I,J,M,N,Q,R). Notably, a smaller but still significant reduction was detected for all markers in both WM regions at E18.5 (Fig. 5A-N), suggesting that the number of OPCs recovers over time even in the absence of ongoing Shh signaling (see below).

To determine whether Shh^{FP} is continually required to block Gli3-R activity during OL specification, we analyzed OPC marker expression in *Shh*$^{\Delta FP/\Delta FP}$;*Gli3*$^{xt/xt}$ double mutants at E15.5. Consistent with earlier stages, there was a substantial rescue of Olig2 expression in the VF of double mutants compared with single *Shh*$^{\Delta FP/\Delta FP}$ mutants (Fig. 4F,G,R). The number of Sox10^{+} and Pdgfrα^{+} OPCs was also significantly greater in *Shh*$^{\Delta FP/\Delta FP}$;*Gli3*$^{xt/xt}$ double versus *Shh*$^{\Delta FP/\Delta FP}$ mutants in both WM regions analyzed (Fig. 4C,G,K,O,Q,R). By contrast, Olig2^{+} cells in the DF decreased even further below the already low number present (Fig. 4B,C,Q). These findings confirm earlier data demonstrating a crucial role for Shh^{FP} in maintaining *Olig2* expression in OPCs by repressing Gli3, and also suggest that later expression of Sox10 and Pdgfrα is similarly maintained by a derepression mechanism, either directly or indirectly, downstream of Olig2 in the VF but not DF. By contrast, the number of Nkx2.2^{+} cells did not differ in *Shh*$^{\Delta FP/\Delta FP}$ embryos in the absence of Gli3 (Fig. 4K,O,Q,R). This finding is consistent with the idea that Shh^{FP} is primarily required to induce Nkx2.2 expression in OPCs via Gli-A proteins (Gli1, 2 or 3) rather than by derepression via inhibition of Gli3-R.

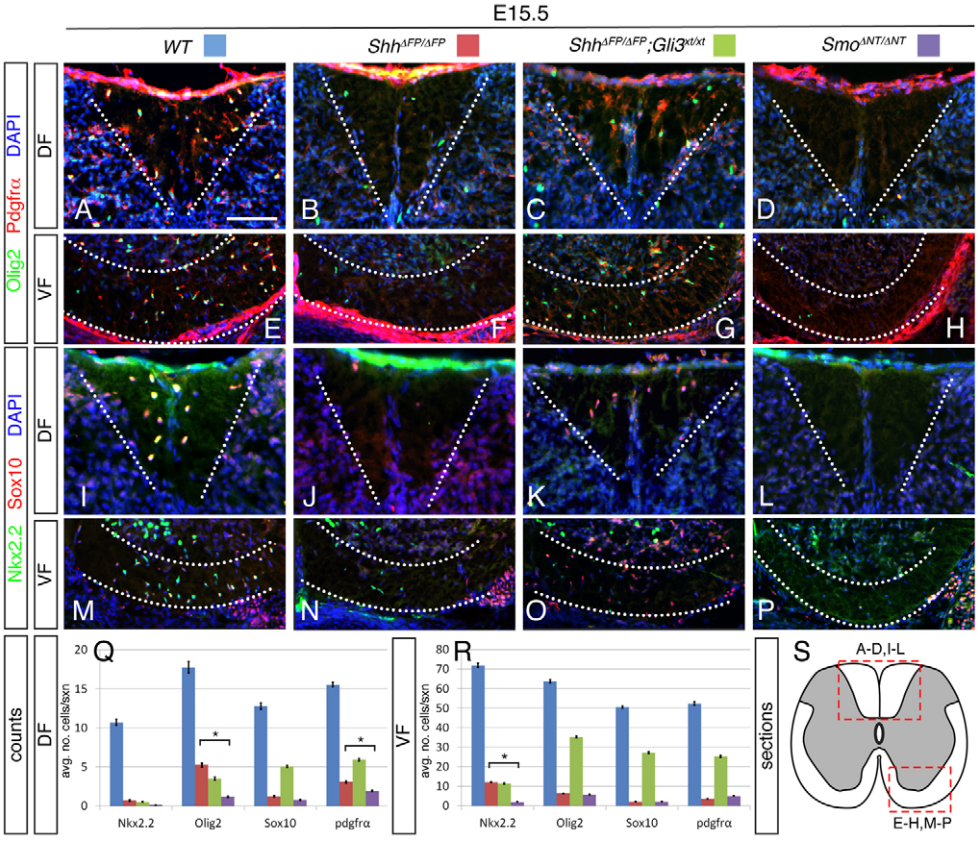

Fig. 4. Altered oligodendrocyte progenitor cell (OPC) marker protein expression in two white matter regions of *Shh*$^{\Delta FP/\Delta FP}$ and *Smo*$^{\Delta NT/\Delta NT}$ embryos at E15.5. (**A-P**) Olig2 and Pdgfrα (A-H) and Nkx2.2 and Sox10 (I-P) expression in the dorsal funiculus (DF) and ventral funiculus (VF) in WT, *Shh*$^{\Delta FP/\Delta FP}$, *Shh*$^{\Delta FP/\Delta FP}$;*Gli3*$^{xt/xt}$ and *Smo*$^{\Delta NT/\Delta NT}$ embryos. Dotted white lines indicate the boundaries of the white matter. (**Q**,**R**) Cell counts for each marker for the indicated genotypes (key above A-D). (**S**) Schematic indicating the area of the spinal cord shown in the panels above. *P<0.05; Student's two-tailed t-test. Error bars indicate s.e.m. Scale bar: 100 μm.

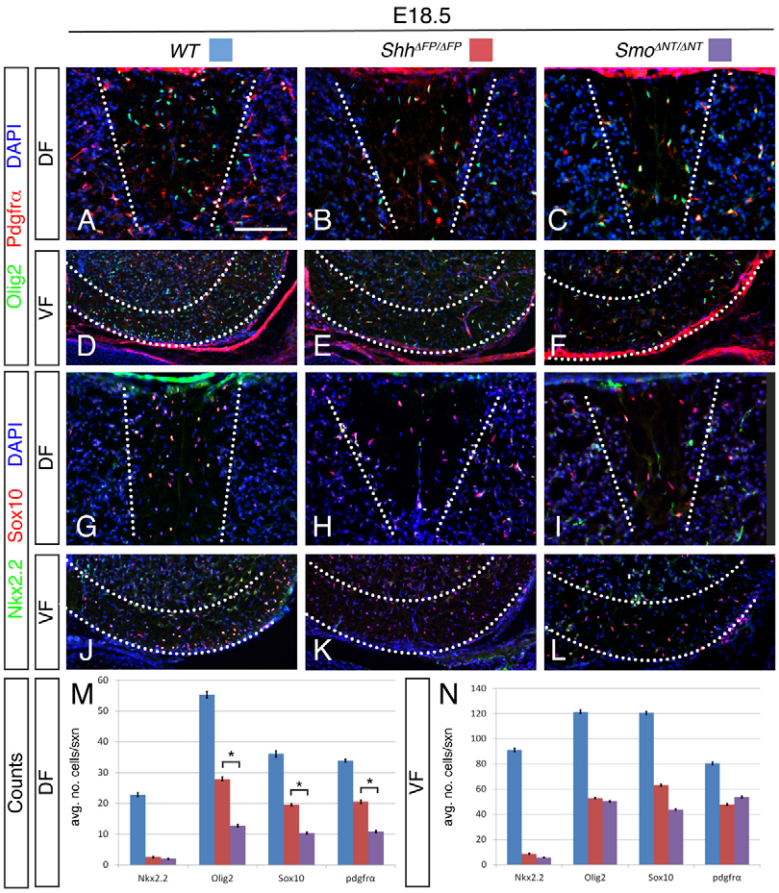

Fig. 5. Altered OPC marker protein expression in two white matter regions of *Shh*$^{\Delta FP/\Delta FP}$ and *Smo*$^{\Delta NT/\Delta NT}$ embryos at E18.5. (**A-L**) Olig2 and Pdgfrα (A-F) and Nkx2.2 and Sox10 (G-L) expression in the dorsal funiculus (DF) and ventral funiculus (VF) in WT, *Shh*$^{\Delta FP/\Delta FP}$ and *Smo*$^{\Delta NT/\Delta NT}$ embryos. Dotted white lines indicate boundaries of white matter regions. (**M**,**N**) Cell counts for each marker for the indicated genotypes. *P<0.0001; Student's two-tailed t-test. Error bars indicate s.e.m. Scale bar: 100 μm.

Oligodendrocyte differentiation is compromised in *Shh*$^{\Delta FP/\Delta FP}$ and *Smo*$^{\Delta NT/\Delta NT}$ mutants

Next, we assayed the requirement of FP-derived Shh for OL differentiation/maturation by examining myelin basic protein (Mbp) expression in *Shh*$^{\Delta FP/\Delta FP}$ and *Smo*$^{\Delta NT/\Delta NT}$ mutants at E18.5 (supplementary material Fig. S7). In WT embryos, Mbp is seen in the VF and DF (n=3 embryos), whereas in *Shh*$^{\Delta FP/\Delta FP}$ mutants there was a decrease in Mbp$^+$ cells in both WM regions (n=3 embryos). Since *Shh*$^{\Delta FP/\Delta FP}$ mutant embryos die at birth, we stained surviving *Smo*$^{\Delta NT/\Delta NT}$ mutants at postnatal day (P) 26 for the mature OL markers Apc, Olig2 and fluoromyelin to determine whether the decrease in embryonic Mbp expression foreshadowed a reduction in OL differentiation and myelination. Although there were 25-30% fewer Apc$^+$ and Olig2$^+$ cells in the DF and 10-15% fewer in the VF in the mutant compared with WT mice, robust fluoromyelin expression was seen (supplementary material Fig. S7D,E). This suggests that OL differentiation and axon tract myelination can occur at near normal levels in mice lacking embryonic Shh signaling within the neural tube, although it may be delayed compared with WT embryos.

To determine whether additional sources of Hh could influence OPC specification during gliogenesis, we again compared marker expression patterns in *Shh*$^{\Delta FP/\Delta FP}$ mutants and *Nestin::Cre;Smo*$^{\Delta NT/\Delta NT}$ embryos at E15.5 and E18.5. The *Nestin::Cre* driver allows all spinal cord OPC populations (both ventral and dorsal derivatives) (Cai et al., 2005; Vallstedt et al., 2005) to be assayed. Again, if other sources of Hh can influence OPC specification during these stages, we would expect a more severe phenotype in *Smo*$^{\Delta NT/\Delta NT}$ than *Shh*$^{\Delta FP/\Delta FP}$ mutants. Indeed, although we found a significant reduction in marker expression in the VF in E15.5 and E18.5 *Smo*$^{\Delta NT/\Delta NT}$ embryos that was similar to or slightly greater than that in *Shh*$^{\Delta FP/\Delta FP}$ mutants (with the exception of Sox10) (Fig. 4H,P,R; Fig. 5D-F,J-L,N), there were notable differences in the DF. Specifically, comparing *Smo*$^{\Delta NT/\Delta NT}$ with *Shh*$^{\Delta FP/\Delta FP}$ mutants, we found significantly fewer Olig2$^+$ and Pdgfrα$^+$, but not Sox10$^+$, OPCs in the DF at E15.5, whereas all three were further reduced at E18.5 in *Smo*$^{\Delta NT/\Delta NT}$ embryos (Fig. 4Q; Fig. 6M). This raises the possibility that an additional source(s) of Hh ligand apart from Shh^{FP} is involved in signaling to OPCs destined to settle in the DF between E15.5 and E18.5. Alternatively, loss of *Smo* in DF OPCs might impact their development independently of Hh signaling.

Evidence for a role for Shh signaling in astrocyte development and function

To investigate the possibility that astrocyte specification and/or differentiation is affected by the absence of intrinsic spinal cord Shh, we first asked whether Hh signaling is ongoing at later embryonic stages in astrocyte progenitors by examining β-gal expression in targeted *Gli1*$^{lacZ/+}$ reporter mice (Bai et al., 2002) at E15.5 and E18.5. In agreement with this possibility, β-gal expression was detected at both stages in a small group of cells in the VZ that also co-expressed Gli2, Nkx6.1 and Pax6 (Fig. 6A-C″; supplementary material Fig. S8; data not shown), and expression was lost in *Shh*$^{\Delta FP/\Delta FP}$ mutants (Fig. 6E,F). Notably, S100 expression (which marks immature and mature astrocytes) was also detected in a small but reproducible number of β-gal$^+$ cells in the VZ, most prominently at E18.5 (Fig. 6D-D″; supplementary material Fig. S8C-C″).

These data indicate active Shh signaling in a subset of S100$^+$ VZ progenitors that generate astrocytes. To test the requirement for this signaling, we examined immature and mature astrocyte marker

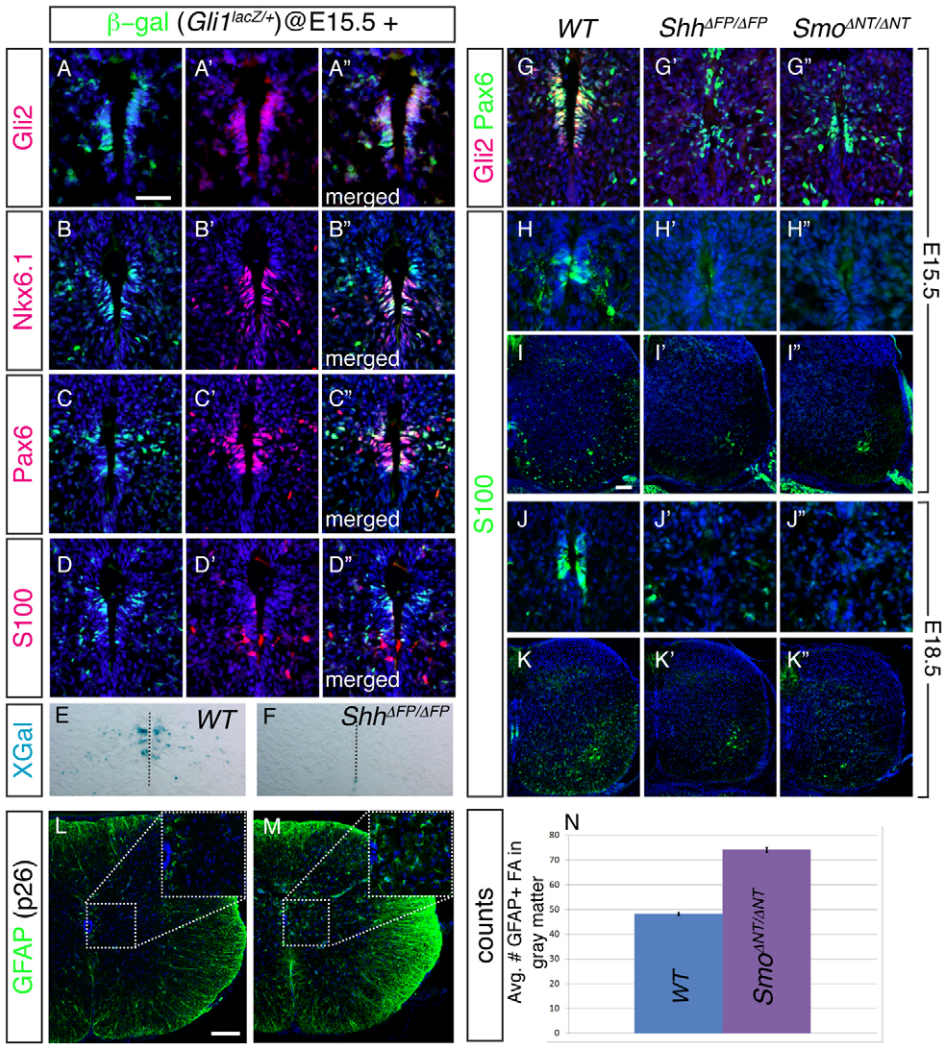

Fig. 6. Expression of Shh-Gli target genes in astrocyte progenitors. (**A-D″**) Co-expression of β-gal from the *Gli1*^{lacZ} reporter line and Gli2 (A), Nkx6.1 (B), Pax6 (C) and S100 (D) at E15.5 in progenitors that will give rise to astrocytes. (A-D) β-Gal; (A′-D′) marker; (A″-D″) merge; all with DAPI. (**E**,**F**) *Gli1*$^{lacZ/+}$ expression is lost in *Shh*$^{\Delta FP/\Delta FP}$ mutants. Dotted line indicates midline. (**G-K″**) Changes in Gli2, Pax6 and S100 expression in *Shh*$^{\Delta FP/\Delta FP}$ and *Smo*$^{\Delta NT/\Delta NT}$ embryos at E15.5 (G-I″) and E18.5 (J-K″). (**L**,**M**) Gfap expression (marking primarily fibrous astrocytes-FA) in WT and *Smo*$^{\Delta NT/\Delta NT}$ mice at P26 in the gray matter region surrounding the central canal (boxed areas). (**N**) Quantification of Gfap expression in the gray matter in WT and *Smo*$^{\Delta NT/\Delta NT}$ mice. Error bars indicate s.e.m. Scale bars: 100 μm.

protein expression in late gestation *Shh*$^{\Delta FP/\Delta FP}$ and postnatal *Smo*$^{\Delta NT/\Delta NT}$ mutants. Notably, expression of both Gli2 and S100 was absent in VZ cells in both genotypes at E15.5 and E18.5 (Fig. 6G-H″,J-J″), and there were many fewer S100^{+} cells in the gray matter at both stages (Fig. 6I-I″,K-K″). By contrast, the number of fibroblast growth factor receptor 3 (*Fgfr3*) or brain lipid binding protein (*Blbp*; *Fabp7* – Mouse Genome Informatics) expressing migrating immature astrocytes did not differ in *Shh*$^{\Delta FP/\Delta FP}$ or *Smo*$^{\Delta NT/\Delta NT}$ embryos at E18.5 compared with WT (data not shown).

To determine whether the changes in S100 expression affected astrocyte differentiation, we examined the expression of glial fibrillary acidic protein (Gfap), which is normally weak or undetectable in protoplasmic (gray matter) but strong in fibrous (white matter) astrocytes. In postnatal *Smo*$^{\Delta NT/\Delta NT}$ mutants, we found that Gfap expression was strongly upregulated in the gray matter region surrounding the central canal compared with WT (Fig. 6L-N). Together, these data provide evidence that intrinsic spinal cord Shh signaling plays a role, directly or indirectly, in astrocyte maturation or function in mice.

Neural tube Hh signaling is required for postnatal ependymal zone cell formation

During normal development, the spinal cord VZ retracts during late gestation due to the terminal division and emigration of progenitor cells following neurogenesis and gliogenesis. The remaining progenitors give rise to ependymal cells lining the central canal [the ependymal zone (EZ)]. Studies tracking progenitor gene expression during this time indicate that adult EZ cells are the descendants of ventral VZ cells originating from the pMN and/or p2 progenitor domains as they retain Nkx6.1 (p3/pMN/p2) but not Nkx2.2 (p3) expression; all other embryonic VZ domains appear to become fully depleted (Fu et al., 2003). The ventral embryonic origin of the adult EZ therefore raises the possibility that cells within this structure develop under the influence of Shh^{FP}. To test this, we examined EZ morphogenesis in *Shh*$^{\Delta FP/\Delta FP}$ and *Smo*$^{\Delta NT/\Delta NT}$ embryos at E15.5, E18.5 and in surviving *Smo*$^{\Delta NT/\Delta NT}$ mutants at P26/30 (*Shh*$^{\Delta FP/\Delta FP}$ mice die at birth).

In WT embryos, the lumen of the VZ begins to close dorsally and ventrally just prior to E15.5 (Fig. 7A). At this stage, vimentin expression is seen in radial processes extending away from the VZ in the position of the future dorsal and ventral/anterior median fissures (Fig. 7A). Cells within the dorsal portion of the remaining VZ region express Pax6 (EZ^{D}), whereas ventral EZ cells (EZ^{V}) are labeled by GFP expression in *Nkx2.2*$^{p3\text{-}CRM}$*::Cre;Rosa*^{GFP} lines that marks only p3 and pMN derivatives (Fig. 7I,K; data not shown) (Wang et al., 2011). This complementary expression pattern is maintained at later embryonic stages and postnatally (Fig. 7I,K). At E18.5, EZ cells begin to form a closely compacted ring surrounding

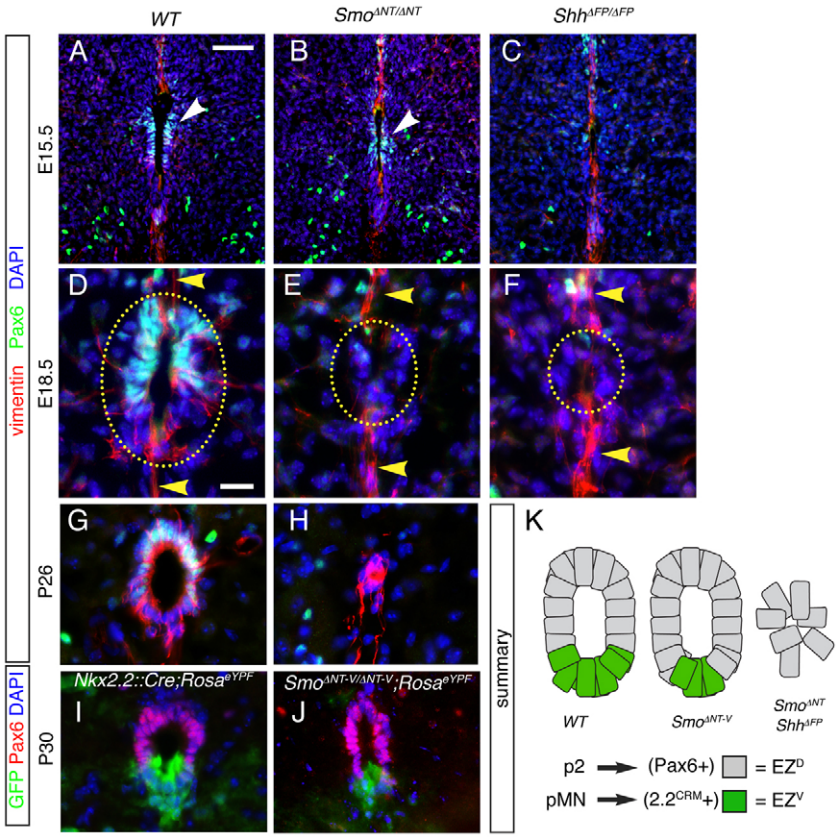

Fig. 7. The spinal cord ependymal zone does not form properly in the absence of late Shh signaling. (**A-F**) Pax6 and vimentin expression in E15.5 (A-C) an E18.5 (D-F) embryos during the formation of the ependymal zone (EZ). In WT embryos, Pax6 expression in the ventricular zone (VZ) (white arrowhead in A, circled area in D) marks the former 'p2' progenitor domain, while the remaining VZ regions (except the pMN domain) become depleted. Pax6 expression is reduced significantly in both $Shh^{\Delta FP/\Delta FP}$ and $Smo^{\Delta NT/\Delta NT}$ embryos (B,C,E,F, white arrowhead and circled areas) and the morphology of cells surrounding the central canal is abnormal. Vimentin staining persists in radial fibers running dorsally and ventrally from the site of the EZ in both WT and mutant embryos (yellow arrowheads). (**G**,**H**) Dorsal EZ cells (marked by vimentin) express Pax6 in P26 mice, whereas in $Smo^{\Delta NT/\Delta NT}$ mice the EZ does not form and no Pax6 expression is detected. (**I**) Expression of Pax6 and β-gal from the $Nkx2.2^{p3\text{-}CRM}$::$Cre;Rosa^{eYFP}$ line is restricted to p3/pMN derivatives that give rise to cells in the ventral portion of the adult EZ, complementing the expression domain of Pax6. (**J**) β-gal and Pax6 expression in embryos in which *Smo* was conditionally inactivated in $Nkx2.2^{p3\text{-}CRM}$-expressing (p3/pMN) cells but not in p2-derived ($Pax6^+$) cells. (**K**) Summary of EZ lineages and phenotype of WT and mutant embryos: p2 derivatives ($Pax6^+$) give rise to cells in the dorsal EZ (EZ^D), while pMN derivatives (expressing the $Nkx2.2^{p3\text{-}CRM}$ reporter) give rise to ventral EZ cells (EZ^V). Scale bars: 100 μm in A-C; 25 μm in D-J.

the central canal (Fig. 7D). Together with published data, these observations suggest that the mature EZ comprises cells with distinct embryonic lineages: an EZ^D derived from the embryonic p2 domain and an EZ^V derived from pMN cells (Fig. 7K). Furthermore, the spatial relationship between these two domains that is established during early neurogenesis is preserved in adulthood (Fig. 7K).

By contrast, in $Shh^{\Delta FP/\Delta FP}$ or $Smo^{\Delta NT/\Delta NT}$ mutants that lack Shh signaling in VZ/EZ cells, Pax6 expression is not seen in EZ^D cells after E15.5 (Fig. 7E-H) and ependymal cells surrounding the central canal do not adopt their normal organization, although radially extending vimentin staining is preserved (Fig. 7E-H). Notably, in $Nkx2.2^{p3\text{-}CRM}$::$Cre;Smo^{-/-}$ $Smo^{\Delta NT\text{-}V;\Delta NT\text{-}V}$ mice, which lack Hh signal transduction only in EZ^V (pMN-derived) but not EZ^D ($Pax6^+$ p2-derived) ependymal cell progenitors, Pax6 expression is maintained and the organization of the EZ is more similar to that of WT, except that the EZ^V domain marked by β-gal expression is reduced (Fig. 7I,J). These data indicate that Hh signaling is required in all developing EZ cells for their proper differentiation, and reveal a novel role for Shh signaling in the formation of this important spinal cord structure in mice.

DISCUSSION

Shh^{FP} is continually required for oligodendrocyte specification and maturation following notochord regression

Our results demonstrate a crucial and unique role for Shh^{FP} signaling within the spinal cord beginning at ~E10.5, as notochord regression is taking place. This is first revealed by the reduction in Olig2 expression in pMN cells at thoracic versus lumbar levels between E10.5 and 11.5 relative to the displacement of the notochord away from the neural tube in these two regions: in $Shh^{\Delta FP/\Delta FP}$ embryos, Olig2 expression is first lost in thoracic regions at E11.5 and then at lumbar levels at E12.5. This correlation suggests that the influence of Shh^{NOTO} diminishes significantly following regression. Consistent with this, Olig2 expression is also absent in embryos lacking *Smo* in neural tube progenitors at stages (E12.5) when the notochord has fully regressed at all axial levels. The similarity in the phenotype in $Shh^{\Delta FP/\Delta FP}$ and $Smo^{\Delta NT/\Delta NT}$ embryos demonstrates that Shh^{NOTO} no longer influences neural tube progenitors following regression, indicating that this event has a significant impact on Shh signaling within the neural tube.

Although it has been shown in a number of studies that OLs produced in the ventral neural tube require Shh signaling, our data supports the idea that the downstream mechanisms differ depending on their specific site of origin. Ventral OLs are generated from two distinct progenitor domains: the Olig2-expressing pMN domain that produces MNs before switching to OLs during gliogenesis, and the Nkx2.2-expressing p3 domain which is located more ventrally, adjacent to the FP (Rowitch, 2004). At E12.5, expression of both Nkx2.2 and Olig2 was reduced in VZ OPCs, with Olig2 being much more severely affected than Nkx2.2. However, since Olig2, but not Nkx2.2, expression is substantially rescued in *Shh;Gli3* double mutants, the maintenance of *Olig2* expression requires the inhibition of Gli3-R formation in pMN/pOlig progenitors. By contrast, the expression of Nkx2.2 in p3 OPCs at E12.5 and in the VF at E15.5 (marking those that originated from the p3 progenitor domain) was not rescued in *Shh;Gli3* double mutants; in fact, fewer cells were seen. Together, these data support the idea that distinct mechanisms are involved in maintaining OPC gene expression in the two subpopulations of ventrally generated OPCs: repression of Gli3-R in pMN/pOlig-derived cells (to allow Olig2 expression) and

formation of Gli-A in p3-derived cells (to induce Nkx2.2). Furthermore, analysis of *Shh;Gli3* double mutants at E15.5 shows that intrinsic CNS Shh signaling is continually required during OL gliogenesis to maintain Olig2 expression in pMN/pOlig-generated OLs via repression of antagonistic Gli3-R activity.

Our analysis of glial progenitor gene expression patterns in *Shh* and *Smo* mutants reveals that the maintenance of both *Fgfbp3* and *Mmd2* requires a similar Shh-Gli3-R derepression mechanism (supplementary material Fig. S6). Interestingly, both of these genes can be linked to Olig2 either functionally or genetically. *Fgfbp3* encodes a member of an extracellular FGF-binding protein family that has been shown to enhance signaling (Tassi et al., 2007; Yamanaka et al., 2011). Thus, reduced expression in *Shh* and *Smo* mutants could in theory lead to attenuation of FGF signaling and reduced Olig2 expression in the spinal cord (Bilican et al., 2008; Novitch et al., 2003). *Mmd2*, which encodes a putative mitochondrial protein involved in energy metabolism and cell proliferation in glial progenitors, was recently identified as a target gene of Sox9/Nfia in the spinal cord, and has been shown to be required for Olig2 expression in chick embryos (Kang et al., 2012). Interestingly, the expression profile of *Mmd2* in *Shh*, *Smo* and *Shh;Gli3* mutants suggests that it might also be directly regulated by Shh-Gli signaling. Consistent with this, a Gli binding site was found in close proximity to the previously identified Sox9 and Nfia binding sites in an *Mmd2* regulatory element (data not shown) (Kang et al., 2012). Together, these data raise the possibility that *Mmd2* is a novel Shh-Gli target gene in spinal cord OPCs.

Intrinsic CNS Shh signaling influences astrocytes

Previous studies have shown that astrocytes are generated from multiple progenitor domains (Rowitch, 2004; Rowitch and Kriegstein, 2010), including the p2 domain in the ventral spinal cord. Despite evidence showing that Hh signaling is required for the V2 neuronal populations that are generated from this domain (Litingtung and Chiang, 2000; Wijgerde et al., 2002), a role for Shh signaling in astrocyte development has not been demonstrated. Astrocytes are the last cell subtype to appear in the CNS; at spinal cord levels, progenitors begin to express astrocyte progenitor markers at ~E15.5. Our data provide several lines of evidence to suggest that Shh-Gli signaling has an important influence on spinal cord astrocytes. First, we find that the Shh transduction factors Gli1 (which is also a target of the canonical pathway) and Gli2 are co-expressed with S100 in E15.5 and E18.5 ‘p2’ astrocyte progenitors (identified by Nkx6.1 and Pax6 expression). Second, expression of Gli1, Gli2 and S100 is absent in *Shh* and *Smo* mutants. Finally, in postnatal *Smo* mutant mice, Gfap expression is strongly upregulated in astrocytes located in the gray matter of the spinal cord.

Our results do not clearly define the mechanisms by which Shh signaling influences spinal cord astrocytes but raise the interesting possibility that regulation of S100 expression might be involved. This secreted calcium-binding protein is expressed predominantly by astrocytes but also by some OLs (Molofsky et al., 2012). Mice lacking S100 develop reactive gliosis, and expression is also downregulated following spinal cord injuries that induce upregulation of Gfap (Chang et al., 2005; Muramatsu et al., 2003). These data support the idea that loss of S100 expression in the absence of Hh signaling results in reactive astrogliosis in postnatal mice. The fact that the expression of astrocyte progenitor markers (*Fgfr3* and *Blbp*) was not substantially altered in *Shh* or *Smo* embryos compared with WT littermates (not shown) indicates, however, that aspects of astrocyte specification can occur even in the absence of Shh. Together with studies showing that loss of Hh signal transduction in adult astrocytes can also lead to a reactive gliosis phenotype (Garcia et al., 2010), these data support an emerging but complex role for Shh in signaling to astrocytes in both embryos and adults.

A role for CNS Hh signaling in normal ependymal zone cell formation

A surprising finding in our study was that the formation of the EZ was severely disrupted in mice lacking embryonic Hh signaling. Despite data showing that the EZ derives solely from the embryonic ventral pMN and p2 progenitor domains (Fu et al., 2003) (this study), a link with Hh signaling had not been explored. Notably, the EZ in rodents has been shown to be an adult stem cell niche that continues to produce primarily glial derivatives under normal circumstances and also following injury in postnatal animals (Johansson et al., 1999; Meletis et al., 2008). Our results indicating a requirement for Hh signaling in establishing this unique germinal zone niche are consistent with similar results in the brain (Machold et al., 2003) and support the possibility that this pathway has a conserved and fundamental role in maintaining adult stem cells in the CNS throughout life.

Acknowledgements

We thank Yuze Shang for expert technical assistance. We are grateful to all the investigators who shared reagents with us.

Funding

This work was funded by the National Institutes of Health [NIH R01 HD057015 and NSF 0131264] and the New Jersey Commission on Spinal Cord Research. Deposited in PMC for release after 12 months.

Competing interests statement

The authors declare no competing financial interests.

Supplementary material

Supplementary material available online at
http://dev.biologists.org/lookup/suppl/doi:10.1242/dev.090845/-/DC1

References

Bai, C. B., Auerbach, W., Lee, J. S., Stephen, D. and Joyner, A. L. (2002). Gli2, but not Gli1, is required for initial Shh signaling and ectopic activation of the Shh pathway. *Development* **129**, 4753-4761.

Bai, C. B., Stephen, D. and Joyner, A. L. (2004). All mouse ventral spinal cord patterning by hedgehog is Gli dependent and involves an activator function of Gli3. *Dev. Cell* **6**, 103-115.

Bilican, B., Fiore-Heriche, C., Compston, A., Allen, N. D. and Chandran, S. (2008). Induction of Olig2 precursors by FGF involves BMP signalling blockade at the Smad level. *PLoS ONE* **3**, e2863.

Borycki, A. G., Brunk, B., Tajbakhsh, S., Buckingham, M., Chiang, C. and Emerson, C. P., Jr (1999). Sonic hedgehog controls epaxial muscle determination through Myf5 activation. *Development* **126**, 4053-4063.

Cai, J., Qi, Y., Hu, X., Tan, M., Liu, Z., Zhang, J., Li, Q., Sander, M. and Qiu, M. (2005). Generation of oligodendrocyte precursor cells from mouse dorsal spinal cord independent of Nkx6 regulation and Shh signaling. *Neuron* **45**, 41-53.

Chamberlain, C. E., Jeong, J., Guo, C., Allen, B. L. and McMahon, A. P. (2008). Notochord-derived Shh concentrates in close association with the apically positioned basal body in neural target cells and forms a dynamic gradient during neural patterning. *Development* **135**, 1097-1106.

Chang, M. S., Ariah, L. M., Marks, A. and Azmitia, E. C. (2005). Chronic gliosis induced by loss of S-100B: knockout mice have enhanced GFAP-immunoreactivity but blunted response to a serotonin challenge. *Brain Res.* **1031**, 1-9.

Chiang, C., Litingtung, Y., Lee, E., Young, K. E., Corden, J. L., Westphal, H. and Beachy, P. A. (1996). Cyclopia and defective axial patterning in mice lacking Sonic hedgehog gene function. *Nature* **383**, 407-413.

Cho, A., Ko, H. W. and Eggenschwiler, J. T. (2008). FKBP8 cell-autonomously controls neural tube patterning through a Gli2- and Kif3a-dependent mechanism. *Dev. Biol.* **321**, 27-39.

Dassule, H. R., Lewis, P., Bei, M., Maas, R. and McMahon, A. P. (2000). Sonic hedgehog regulates growth and morphogenesis of the tooth. *Development* **127**, 4775-4785.

Deneen, B., Ho, R., Lukaszewicz, A., Hochstim, C. J., Gronostajski, R. M. and Anderson, D. J. (2006). The transcription factor NFIA controls the onset of gliogenesis in the developing spinal cord. *Neuron* **52**, 953-968.
Dessaud, E., McMahon, A. P. and Briscoe, J. (2008). Pattern formation in the vertebrate neural tube: a sonic hedgehog morphogen-regulated transcriptional network. *Development* **135**, 2489-2503.
Dessaud, E., Ribes, V., Balaskas, N., Yang, L. L., Pierani, A., Kicheva, A., Novitch, B. G., Briscoe, J. and Sasai, N. (2010). Dynamic assignment and maintenance of positional identity in the ventral neural tube by the morphogen sonic hedgehog. *PLoS Biol.* **8**, e1000382.
Ding, Q., Motoyama, J., Gasca, S., Mo, R., Sasaki, H., Rossant, J. and Hui, C. C. (1998). Diminished Sonic hedgehog signaling and lack of floor plate differentiation in Gli2 mutant mice. *Development* **125**, 2533-2543.
Fu, H., Qi, Y., Tan, M., Cai, J., Hu, X., Liu, Z., Jensen, J. and Qiu, M. (2003). Molecular mapping of the origin of postnatal spinal cord ependymal cells: evidence that adult ependymal cells are derived from Nkx6.1+ ventral neural progenitor cells. *J. Comp. Neurol.* **456**, 237-244.
Garcia, A. D., Petrova, R., Eng, L. and Joyner, A. L. (2010). Sonic hedgehog regulates discrete populations of astrocytes in the adult mouse forebrain. *J. Neurosci.* **30**, 13597-13608.
Hui, C. C. and Joyner, A. L. (1993). A mouse model of greig cephalopolysyndactyly syndrome: the extra-toesJ mutation contains an intragenic deletion of the Gli3 gene. *Nat. Genet.* **3**, 241-246.
Jacob, J. and Briscoe, J. (2003). Gli proteins and the control of spinal-cord patterning. *EMBO Rep.* **4**, 761-765.
Jeong, J. and McMahon, A. P. (2005). Growth and pattern of the mammalian neural tube are governed by partially overlapping feedback activities of the hedgehog antagonists patched 1 and Hhip1. *Development* **132**, 143-154.
Jessell, T. M. (2000). Neuronal specification in the spinal cord: inductive signals and transcriptional codes. *Nat. Rev. Genet.* **1**, 20-29.
Johansson, C. B., Momma, S., Clarke, D. L., Risling, M., Lendahl, U. and Frisén, J. (1999). Identification of a neural stem cell in the adult mammalian central nervous system. *Cell* **96**, 25-34.
Kang, P., Lee, H. K., Glasgow, S. M., Finley, M., Donti, T., Gaber, Z. B., Graham, B. H., Foster, A. E., Novitch, B. G., Gronostajski, R. M. et al. (2012). Sox9 and NFIA coordinate a transcriptional regulatory cascade during the initiation of gliogenesis. *Neuron* **74**, 79-94.
Lei, Q., Zelman, A. K., Kuang, E., Li, S. and Matise, M. P. (2004). Transduction of graded Hedgehog signaling by a combination of Gli2 and Gli3 activator functions in the developing spinal cord. *Development* **131**, 3593-3604.
Lei, Q., Jeong, Y., Misra, K., Li, S., Zelman, A. K., Epstein, D. J. and Matise, M. P. (2006). Wnt signaling inhibitors regulate the transcriptional response to morphogenetic Shh-Gli signaling in the neural tube. *Dev. Cell* **11**, 325-337.
Litingtung, Y. and Chiang, C. (2000). Specification of ventral neuron types is mediated by an antagonistic interaction between Shh and Gli3. *Nat. Neurosci.* **3**, 979-985.
Long, F., Zhang, X. M., Karp, S., Yang, Y. and McMahon, A. P. (2001). Genetic manipulation of hedgehog signaling in the endochondral skeleton reveals a direct role in the regulation of chondrocyte proliferation. *Development* **128**, 5099-5108.
Lu, Q. R., Sun, T., Zhu, Z., Ma, N., Garcia, M., Stiles, C. D. and Rowitch, D. H. (2002). Common developmental requirement for Olig function indicates a motor neuron/oligodendrocyte connection. *Cell* **109**, 75-86.
Machold, R., Hayashi, S., Rutlin, M., Muzumdar, M. D., Nery, S., Corbin, J. G., Gritli-Linde, A., Dellovade, T., Porter, J. A., Rubin, L. L. et al. (2003). Sonic hedgehog is required for progenitor cell maintenance in telencephalic stem cell niches. *Neuron* **39**, 937-950.
Maka, M., Stolt, C. C. and Wegner, M. (2005). Identification of Sox8 as a modifier gene in a mouse model of Hirschsprung disease reveals underlying molecular defect. *Dev. Biol.* **277**, 155-169.
Matise, M. P. and Wang, H. (2011). Sonic hedgehog signaling in the developing CNS where it has been and where it is going. *Curr. Top. Dev. Biol.* **97**, 75-117.
Matise, M. P., Epstein, D. J., Park, H. L., Platt, K. A. and Joyner, A. L. (1998). Gli2 is required for induction of floor plate and adjacent cells, but not most ventral neurons in the mouse central nervous system. *Development* **125**, 2759-2770.
Meletis, K., Barnabé-Heider, F., Carlén, M., Evergren, E., Tomilin, N., Shupliakov, O. and Frisén, J. (2008). Spinal cord injury reveals multilineage differentiation of ependymal cells. *PLoS Biol.* **6**, e182.
Molofsky, A. V., Krencik, R., Ullian, E. M., Tsai, H. H., Deneen, B., Richardson, W. D., Barres, B. A. and Rowitch, D. H. (2012). Astrocytes and disease: a neurodevelopmental perspective. *Genes Dev.* **26**, 891-907.
Muramatsu, Y., Kurosaki, R., Watanabe, H., Michimata, M., Matsubara, M., Imai, Y. and Araki, T. (2003). Expression of S-100 protein is related to neuronal damage in MPTP-treated mice. *Glia* **42**, 307-313.
Novitch, B. G., Wichterle, H., Jessell, T. M. and Sockanathan, S. (2003). A requirement for retinoic acid-mediated transcriptional activation in ventral neural patterning and motor neuron specification. *Neuron* **40**, 81-95.
Pan, Y. and Wang, B. (2007). A novel protein-processing domain in Gli2 and Gli3 differentially blocks complete protein degradation by the proteasome. *J. Biol. Chem.* **282**, 10846-10852.
Pan, Y., Bai, C. B., Joyner, A. L. and Wang, B. (2006). Sonic hedgehog signaling regulates Gli2 transcriptional activity by suppressing its processing and degradation. *Mol. Cell. Biol.* **26**, 3365-3377.
Rallu, M., Machold, R., Gaiano, N., Corbin, J. G., McMahon, A. P. and Fishell, G. (2002). Dorsoventral patterning is established in the telencephalon of mutants lacking both Gli3 and Hedgehog signaling. *Development* **129**, 4963-4974.
Rowitch, D. H. (2004). Glial specification in the vertebrate neural tube. *Nat. Rev. Neurosci.* **5**, 409-419.
Rowitch, D. H. and Kriegstein, A. R. (2010). Developmental genetics of vertebrate glial-cell specification. *Nature* **468**, 214-222.
Sasaki, H. and Hogan, B. L. (1996). Enhancer analysis of the mouse HNF-3 beta gene: regulatory elements for node/notochord and floor plate are independent and consist of multiple sub-elements. *Genes Cells* **1**, 59-72.
Soriano, P. (1999). Generalized lacZ expression with the ROSA26 Cre reporter strain. *Nat. Genet.* **21**, 70-71.
Srinivas, S., Watanabe, T., Lin, C. S., William, C. M., Tanabe, Y., Jessell, T. M. and Costantini, F. (2001). Cre reporter strains produced by targeted insertion of EYFP and ECFP into the ROSA26 locus. *BMC Dev. Biol.* **1**, 4.
Stolt, C. C., Lommes, P., Sock, E., Chaboissier, M. C., Schedl, A. and Wegner, M. (2003). The Sox9 transcription factor determines glial fate choice in the developing spinal cord. *Genes Dev.* **17**, 1677-1689.
Tassi, E., Walter, S., Aigner, A., Cabal-Manzano, R. H., Ray, R., Reier, P. J. and Wellstein, A. (2007). Effects on neurite outgrowth and cell survival of a secreted fibroblast growth factor binding protein upregulated during spinal cord injury. *Am. J. Physiol. Regul. Integr. Comp. Physiol.* **293**, R775-R783.
Tronche, F., Kellendonk, C., Kretz, O., Gass, P., Anlag, K., Orban, P. C., Bock, R., Klein, R. and Schütz, G. (1999). Disruption of the glucocorticoid receptor gene in the nervous system results in reduced anxiety. *Nat. Genet.* **23**, 99-103.
Vallstedt, A., Klos, J. M. and Ericson, J. (2005). Multiple dorsoventral origins of oligodendrocyte generation in the spinal cord and hindbrain. *Neuron* **45**, 55-67.
Wang, H., Lei, Q., Oosterveen, T., Ericson, J. and Matise, M. P. (2011). Tcf/Lef repressors differentially regulate Shh-Gli target gene activation thresholds to generate progenitor patterning in the developing CNS. *Development* **138**, 3711-3721.
Wen, X., Lai, C. K., Evangelista, M., Hongo, J. A., de Sauvage, F. J. and Scales, S. J. (2010). Kinetics of hedgehog-dependent full-length Gli3 accumulation in primary cilia and subsequent degradation. *Mol. Cell Biol.* **30**, 1910-1922.
Wijgerde, M., McMahon, J. A., Rule, M. and McMahon, A. P. (2002). A direct requirement for Hedgehog signaling for normal specification of all ventral progenitor domains in the presumptive mammalian spinal cord. *Genes Dev.* **16**, 2849-2864.
Yamanaka, Y., Kitano, A., Takao, K., Prasansuklab, A., Mushiroda, T., Yamazaki, K., Kumada, T., Shibata, M., Takaoka, Y., Awaya, T. et al. (2011). Inactivation of fibroblast growth factor binding protein 3 causes anxiety-related behaviors. *Mol. Cell. Neurosci.* **46**, 200-212.

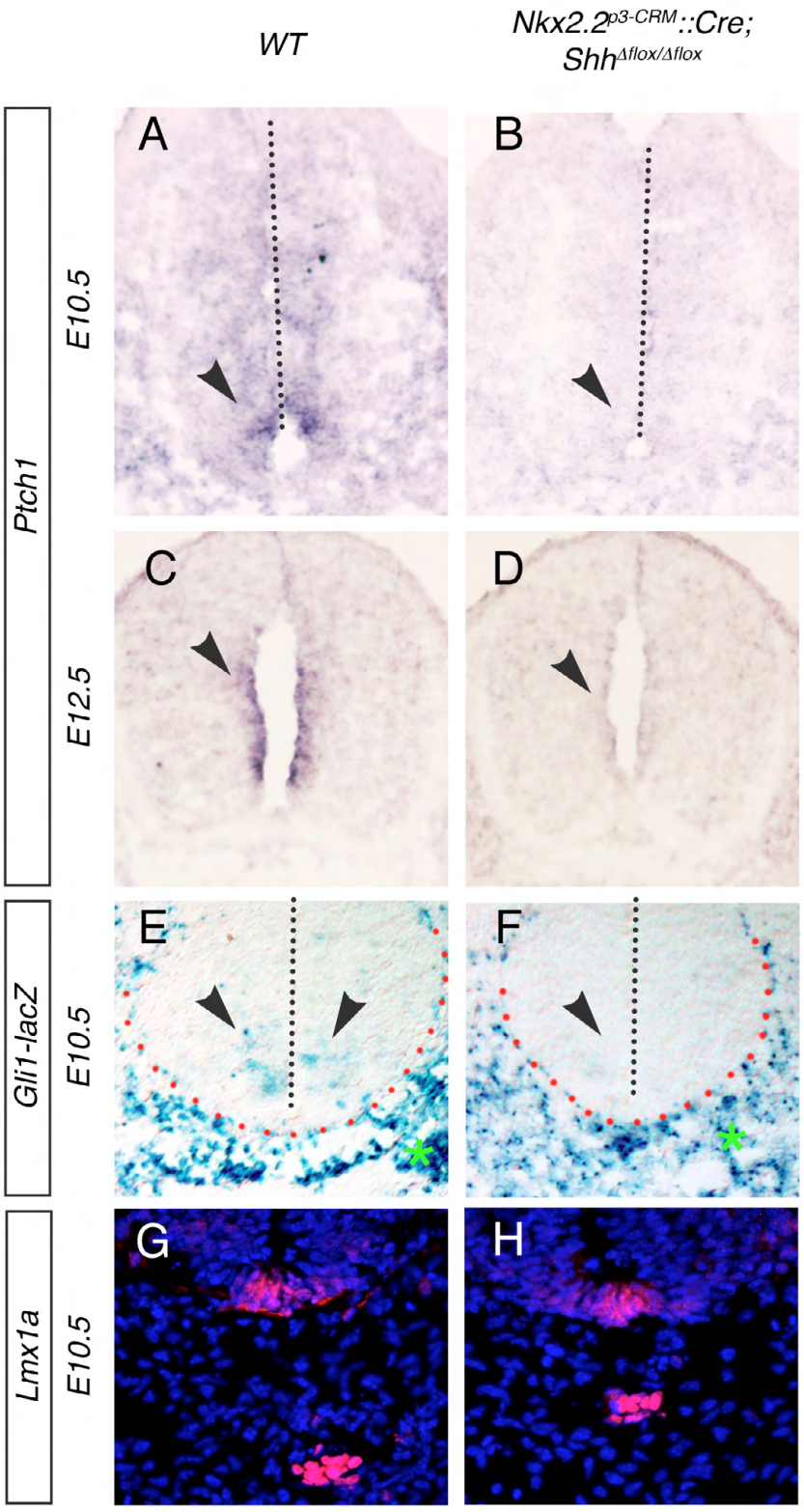

Fig. S1. Shh target gene expression changes in the neural tube of *Shh*$^{\Delta FP/\Delta FP}$ embryos. (**A-D**) *Ptch1* expression is reduced at both E10.5 and E12.5 (arrowheads). (**E**,**F**) β-gal expression in a targeted *Gli1*^{lacZ} reporter line shows weaker expression in the ventral spinal cord in *Shh*$^{\Delta FP/\Delta FP}$ embryos (arrowheads) at E10.5. (**G**,**H**) Lmx1a expression is not altered in the FP at E10.5. Section in H is at a more rostral level than that in G in the thoracic region.

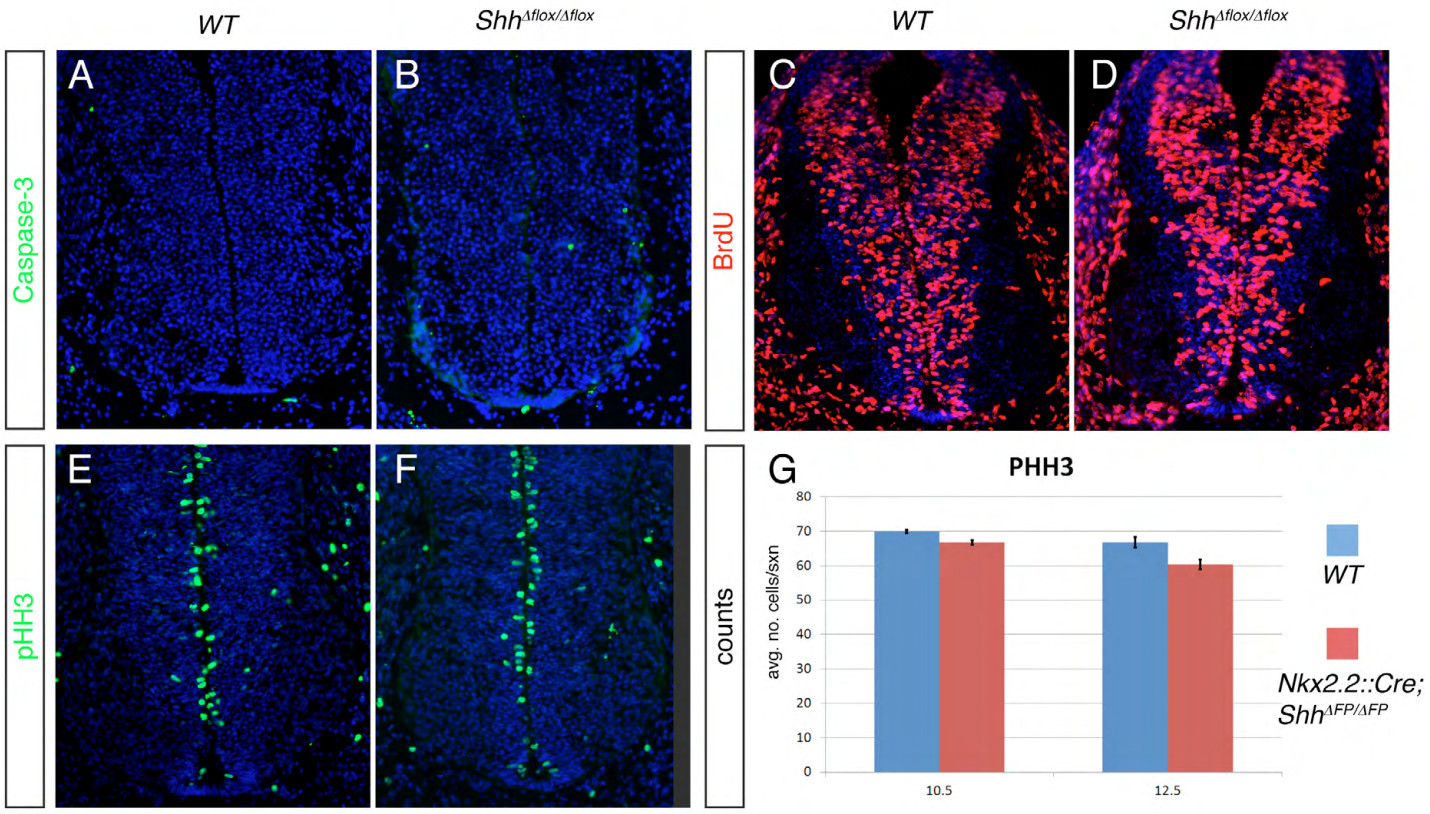

Fig. S2. Analysis of cell proliferation and cell death in *Shh*$^{\Delta FP/\Delta FP}$ embryos. (**A**,**B**) Activated caspase 3 expression is not elevated in conditional mutants compared with WT. (**C-G**) No significant differences were seen in BrdU incorporation rates or pHH3 expression in *Nkx2.2*$^{p3\text{-}CRM}$*::Cre;Shh*$^{\Delta FP/\Delta FP}$ conditional mutants at E10.5 (A-F) and E12.5 (G) compared with WT.

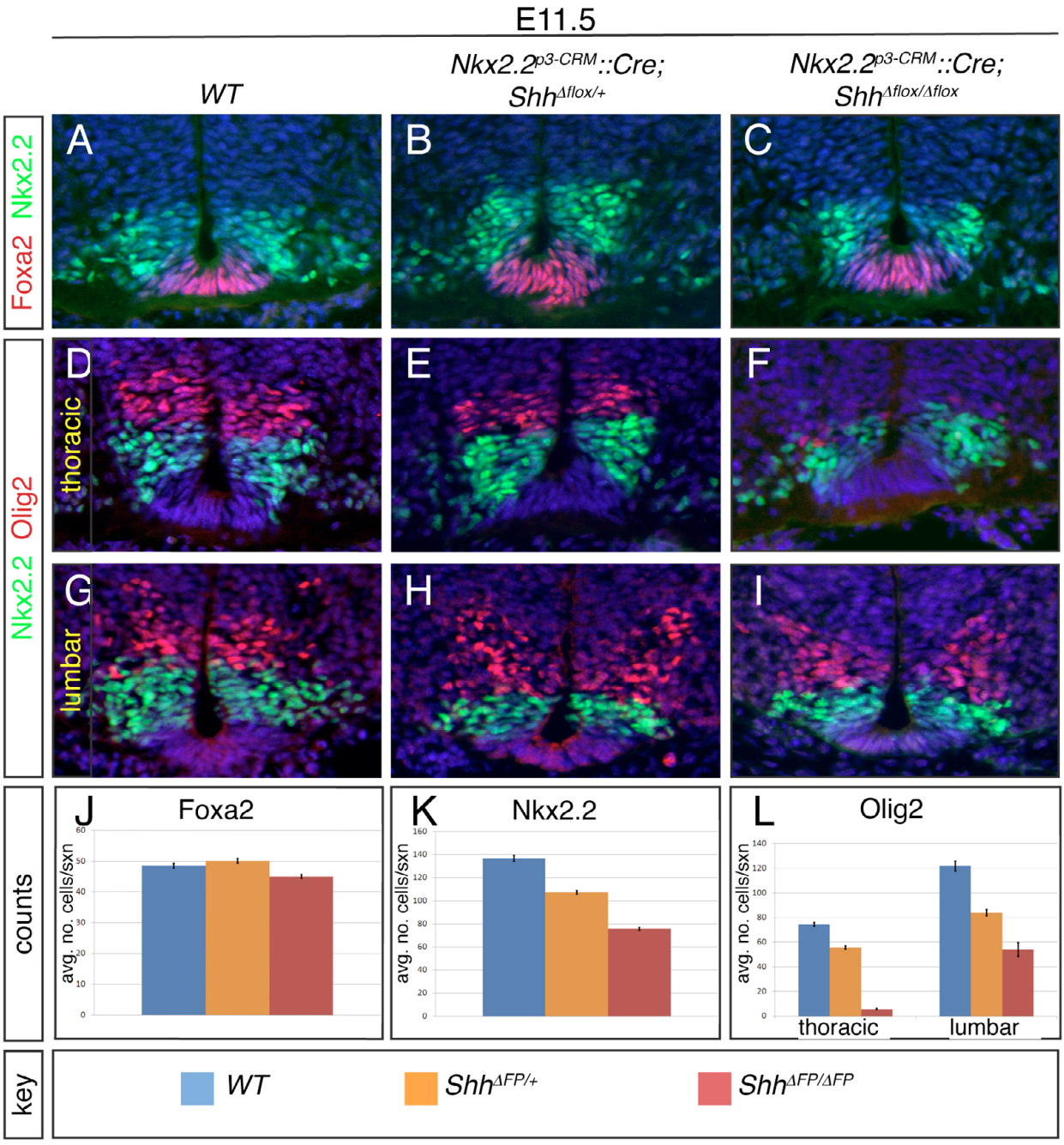

Fig. S3. Altered progenitor domain marker protein expression in *Shh*$^{\Delta FP/\Delta FP}$ embryos at E11.5. (**A-C**) Foxa2 and Nkx2.2 expression in WT (A), *Shh*$^{\Delta FP/+}$ heterozygotes (B) and *Shh*$^{\Delta FP/\Delta FP}$ homozygotes (C). (**D-I**) Nkx2.2 and Olig2 expression in thoracic (D-F) and lumbar (G-I) regions. (**J-L**) Quantification of marker expression.

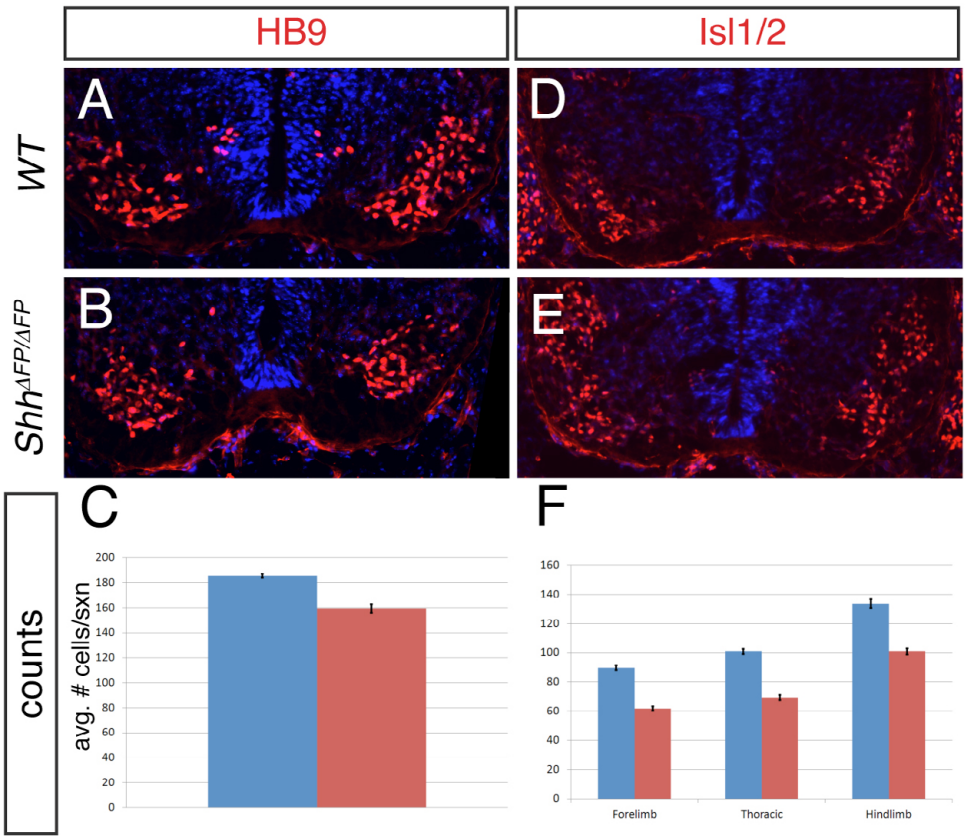

Fig. S4. Reduction in motoneuron formation in *Shh*$^{\Delta FP/\Delta FP}$ embryos. Staining for postmitotic motoneuron markers HB9 (**A-C**) and Isl1/2 (**D-F**) in E12.5 embryos shows that reduced numbers of cells are generated.

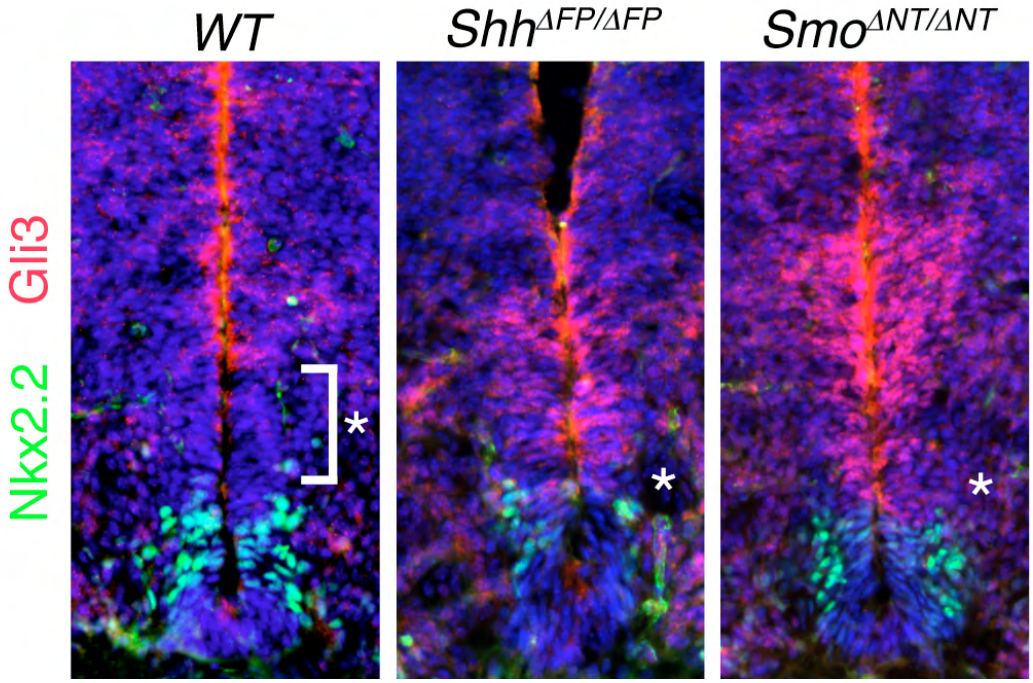

Fig. S5. Gli3 expression shifts ventrally in *Shh*$^{\Delta FP/\Delta FP}$ and *Smo*$^{\Delta NT/\Delta NT}$ embryos. E11.5 embryos stained for Gli3 and Nkx2.2 (marking the p3 domain) show a ventral shift in the expression boundary of Gli3 into the pMN domain (brackets, asterisks).

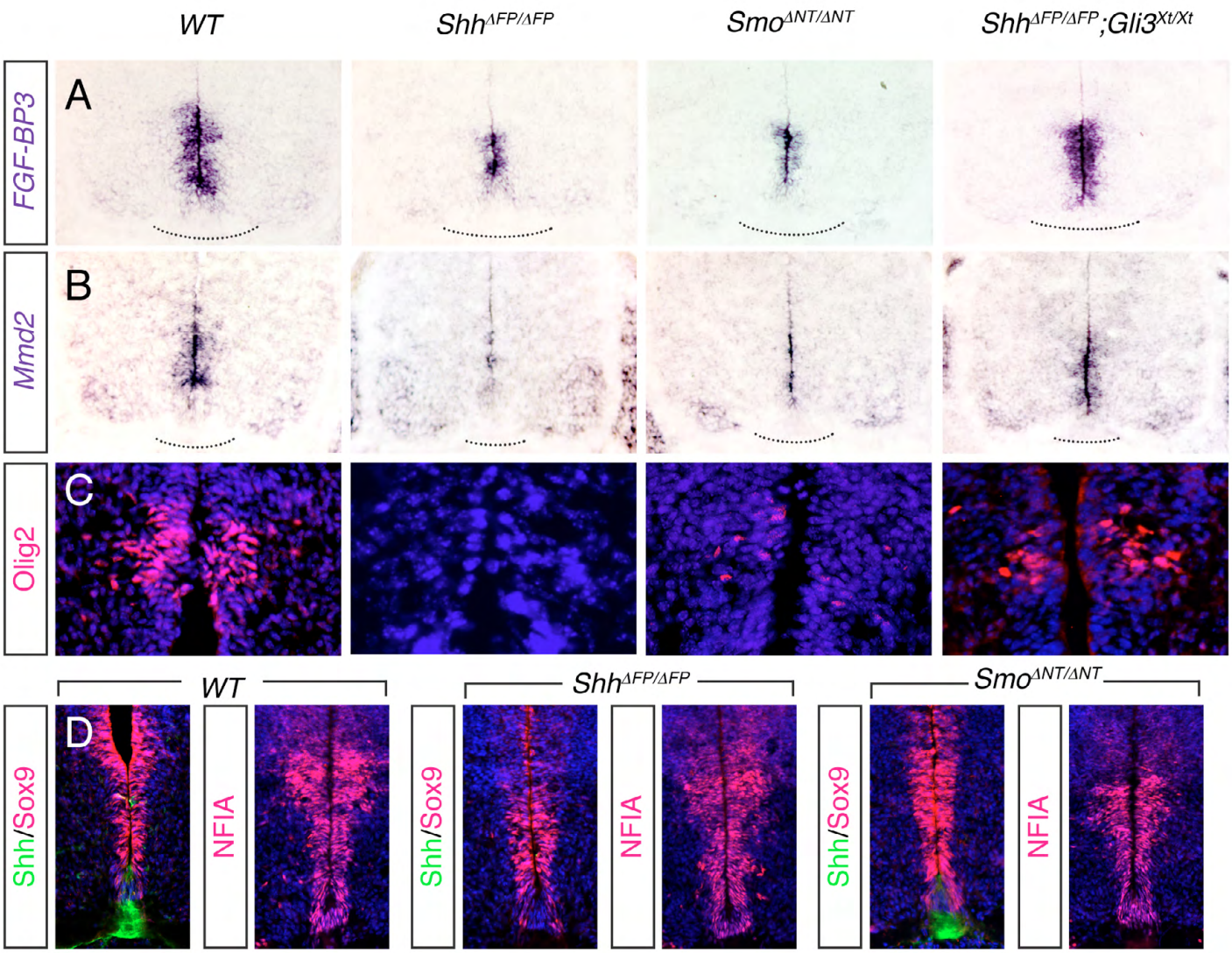

Fig. S6. Changes in the expression of specific glial progenitor genes in mutant embryos identifies novel Shh-Gli target genes. (**A**,**B**) Staining for Fgfbp3 and Mmd2 in WT, *Shh*$^{\Delta FP/\Delta FP}$, *Smo*$^{\Delta NT/\Delta N}$ and *Shh*$^{\Delta FP/\Delta FP}$*;Gli3*$^{xt/xt}$ mutant embryos at E12.5. Expression of both genes is reduced or absent in *Shh*$^{\Delta FP/\Delta FP}$ and *Smo*$^{\Delta NT/\Delta NT}$ embryos but is restored in *Shh*$^{\Delta FP/\Delta FP}$*;Gli3*$^{xt/xt}$ mutants. (**C**) Expression of Olig2, a gene that appears to be primarily regulated by Gli3 derepression, is shown for comparison. (**D**) Sox9 and Nfia expression in *Shh*$^{\Delta FP/\Delta FP}$ and *Smo*$^{\Delta NT/\Delta NT}$ embryos is not altered. Shh is shown in some panels for comparison.

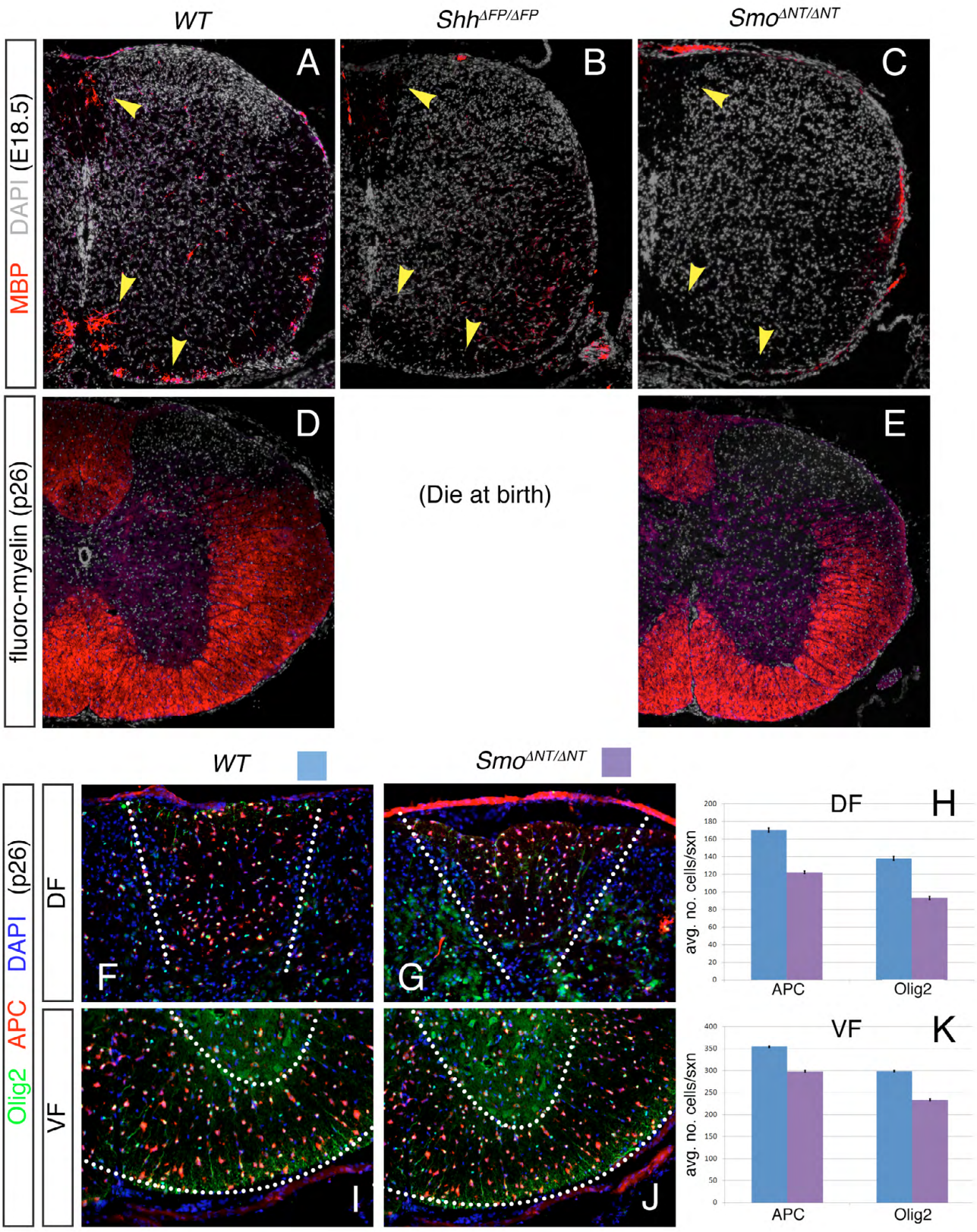

Fig. S7. Expression of differentiated OL marker protein expression in *Shh*$^{\Delta FP/\Delta FP}$ and *Smo*$^{\Delta NT/\Delta NT}$ embryos at E18.5 and P26. (**A-C**) Myelin basic protein (Mbp) expression in WT (A), *Shh*$^{\Delta FP/\Delta FP}$ (B) and *Smo*$^{\Delta NT/\Delta NT}$ (C) embryos shows reduced staining in both the VF and DF in mutant embryos (arrowheads). (**D**,**E**) Fluoromyelin expression is similar in WT (D) and *Smo*$^{\Delta NT/\Delta NT}$ (E) mice at P26. (**F-K**) Analysis of differentiated OL marker protein expression in P26 *Smo*$^{\Delta NT/\Delta NT}$ mice. Both Olig2 and Apc are reduced in both the DF and VF at this stage but to a lesser degree than at embryonic stages.

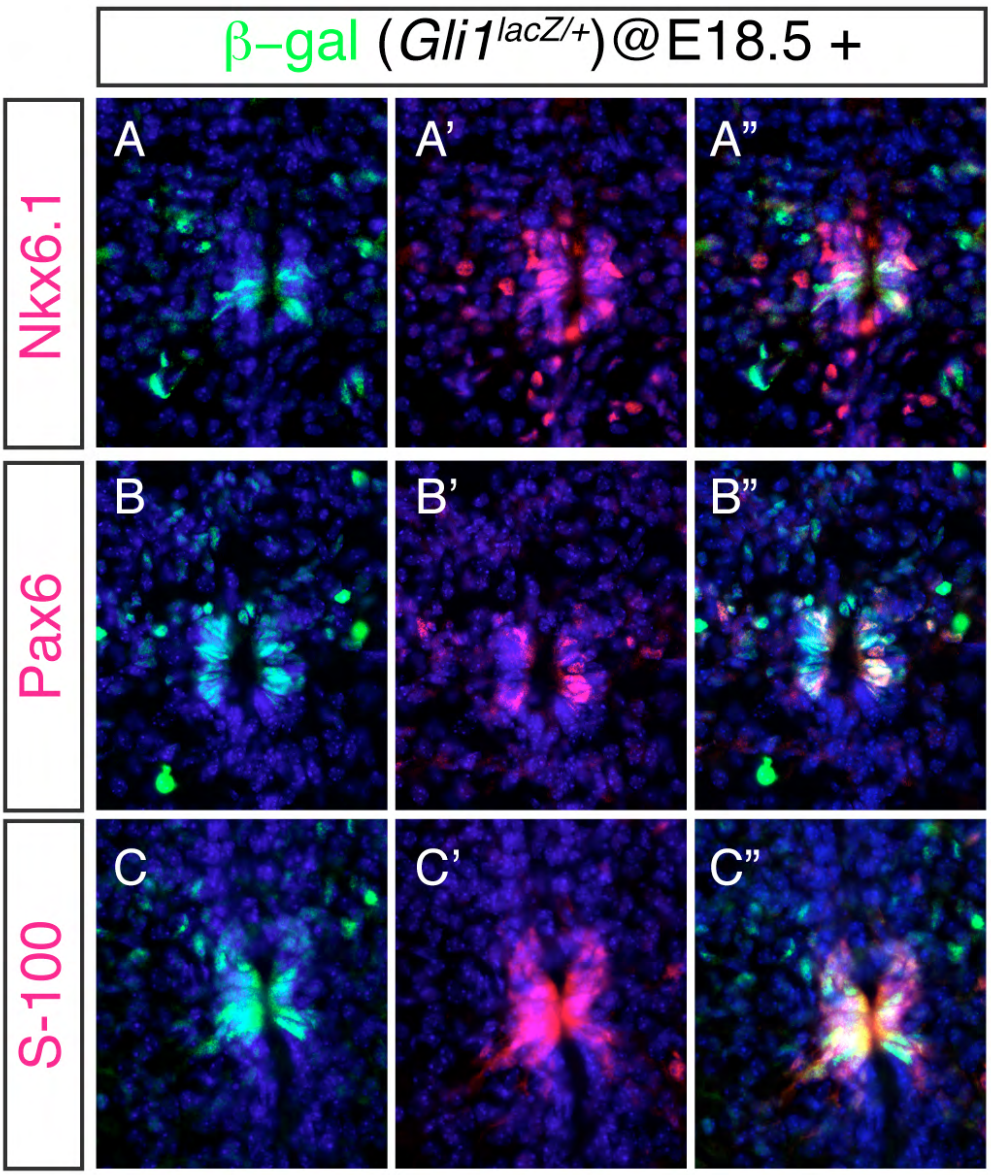

Fig. S8. Co-expression of Nkx6.1, Pax6 and S-100 in Gli1-lacZ^{+} VZ cells at E18.5. (**A-C″**) All three markers show strong overlap with β-gal (from a *Gli1^{lacZ}* knock-in line) in VZ cells (yellow). (A-C) β-gal; (A′-C′) marker; (A″-C″) merge; all with DAPI.